

Analytic Spectra of CMB Anisotropies and Polarization Generated by Scalar Perturbations in Synchronous Gauge

Z. Cai^{1,2,3*}, Y. Zhang^{1 †},

¹ Key Laboratory for Researches in Galaxies and Cosmology,
Department of Astronomy, University of Science and Technology of China,
Hefei, Anhui, 230026, China

² Department of Physics, University of Arizona, Tucson, AZ 85721, USA

³ Steward Observatory, University of Arizona, Tucson, AZ, 85721, USA

Abstract

The temperature anisotropies and polarization of the cosmic microwave background radiation (CMB) not only serve as indispensable cosmological probes, but also provide a unique channel to detect relic gravitational waves (RGW) at very long wavelengths. Analytical studies of the anisotropies and polarization improve our understanding of various cosmic processes and help to separate the contribution of RGW from that of density perturbations.

We present a detailed analytical calculation of CMB temperature anisotropies α_k and polarization β_k generated by scalar metric perturbations in synchronous gauge, parallel to our previous work with RGW as a generating source. This is realized primarily by an analytic time-integration of Boltzmann's equation, yielding the closed forms of α_k and β_k . Approximations, such as the tight-coupling approximation for photons a prior to the recombination and the long wavelength limit for scalar perturbations are used. The residual gauge modes in scalar perturbations are analyzed and a proper joining condition of scalar perturbations at the radiation-matter equality is chosen, ensuring the continuity of energy perturbation.

The resulting analytic expressions of the multipole moments of polarization a_l^E , and of temperature anisotropies a_l^T are explicit functions of the scalar perturbations, recombination time, recombination width, photon free streaming damping factor, baryon fraction, initial amplitude, primordial scalar spectral index, and the running index. These results show that a longer recombination width yields higher amplitudes of polarization on large scales and more damping on small scales, and that a late recombination time shifts the peaks of $C_l^{XX'}$ to larger angular scales.

*caiz at email.arizona.edu

†yzh at ustc.edu.cn

Calculations show that a_l^E is generated in the presence of the quadrupole α_2 of temperature anisotropies via scattering, both having similar structures and being smaller than the total a_l^T , which consists of the contributions from the monopole, dipole, quadrupole, and Sachs-Wolfe terms as well. The origin of the two bumps in C_l^{EE} on large angular scales is found to be due to the time derivative of the monopole of temperature anisotropies. Furthermore, a_l^E together with a_l^T demonstrates explicitly that the peaks of C_l^{EE} and C_l^{TT} alternate in l -space. These results substantially extend earlier analytic work.

The analytic spectra $C_l^{XX'}$ agree with the numerical ones and with those observed by WMAP on large scales ($l \lesssim 500$), but deviate considerably from the numerical results on smaller scales, showing the limitations of our approximate analytic calculations. Several possible improvements are pointed out for further studies.

PACS number: 98.70.Vc, 98.80.-k, 98.80.Jk,

Key words: cosmic microwave background radiation, scalar perturbations, polarizations

1. Introduction

By confronting predictions of theoretical cosmological models with the data on the CMB by the observations, such as BOOMERANG [1], MAXIMA [2], DASI [3], WMAP [4, 5, 6, 7, 8, 9], Archeops [10], CBI [11], QUaD [12], BICEP [13] etc, several important cosmological parameters of the standard Big Bang model have been directly measured or constrained. These studies have been instrumental for rapid progresses toward understanding of the evolution of the Universe, and for the advent of an epoch of precise cosmology.

On the side of theory, these achievements have been possible through detailed computations of the spectra of the CMB temperature anisotropies and polarizations. Codes of numerical computation, such as CMBFAST [14] and CAMB [15], give the the spectra $C_l^{XX'}$ of CMB temperature anisotropies and polarizations. The prominent structure of $C_l^{XX'}$ involves various cosmological parameters, as it depends upon several major physical processes during the cosmic expansion, such as the inflation, radiation-matter equality, recombination, and the reionization as well. Analytical studies are still indispensable for understanding how various underlying physical effects give rise to the observed behavior and for theoretical interpretations of the observational data. In particular, the analytical spectra are helpful in revealing their explicit dependence on the cosmological parameters and possible degeneracies between them. So it would be desired to have the analytical $C_l^{XX'}$ for a better understanding of physics of CMB.

From computational point of view, the CMB temperature anisotropies and polarizations are determined by the Boltzmann's equation of the photon gas in the expanding Universe. Although a number of ingredients will influence this equation, two key elements are responsible for the overall features of $C_l^{XX'}$, i.e., Thompson scattering during the recombination process around a redshift $z \sim 1000$ and the metric perturbations h_{ij} of Robertson-Walker spacetime entering the equation as the Sachs-Wolfe term [16]. Generally, there are two types of metric perturbations as the source: the scalar (density) perturbations [17, 18, 19] and the tensorial perturbations, i.e., RGW [20, 21, 22]. Both types can be generated during early stages of the universe, such as the inflationary expansion. Among them, the contribution from scalar perturbations is believed to be dominant over that from RGW [23, 24, 25, 26, 27, 28, 29, 30], characterized by a tensor/scalar ratio r [31, 32]. For a power law spectrum of the primordial fluctuations, WMAP5 data alone puts an upper limit on the ratio $r < 0.55$ (95% CL) [7], while WMAP7 gives $r < 0.49$ (95% CL) for Λ CDM+Tensors+Running [8]. The recent data of LIGO S5 [33] with cross-correlation of H1 and L1 gives a constraint $r < 0.55$ for the flat primordial tensorial perturbations with a negligible running index [34]. For the case of RGW as the source, Refs. [35, 36] derived the analytical spectrum C_l^{TT} of temperature anisotropies, and Ref. [37] gave all four analytical spectra C_l^{EE} , C_l^{BB} , C_l^{TE} , as well as C_l^{TT} . Ref. [38] incorporated the reionization process into calculation and obtained the reionized analytical spectra $C_l^{XX'}$.

Ref.[39] presented a fully covariant and gauge-invariant formulation of Boltzmann's equations. The analytic calculation of the scalar induced C_l^{TT} was made in Newtonian (longitudinal) gauge in Refs [40, 41]. Ref.[42] gives an analysis of C_l^{TT} in synchronous gauge, but the treatment of temperature anisotropies itself was not enough to separate contributions of monopole, dipole, quadrupole, and Sachs-Wolfe terms. It did not address the CMB polarizations either. Ref.[43] gave a unifying framework in synchronous gauge to discuss the scalar induced spectra C_l^{TT} , C_l^{EE} , C_l^{TE} and as well as the RGW induced spectra $C_l^{XX'}$. Motivated by possible extractions of signals of RGW using anti-correlation of C_l^{TE} , attempts were made to estimate qualitatively the possible forms of multipoles a_l^T of the temperature anisotropies and a_l^E of the polarization at $l \sim 50$ [43]. However, the analysis was still preliminary by lacking of an explicit formula of a_l^T , since the time-integrations of the Boltzmann's equation as a key procedure was not carried out. Viewing these, in this paper, we shall perform a detailed, analytic calculation of a_l^T and a_l^E induced by the scalar perturbations in synchronous gauge, and present the analytical spectra $C_l^{XX'}$, which will be at the same level of accuracy as the analytical $C_l^{XX'}$ by RGW [36, 37, 38]. Aside several new insights into the physics of CMB, in particular, our resulting cross-correlation spectrum C_l^{TE} has already demonstrated some inaccuracy in the preliminary analysis of Ref.[43]. Therefore, these two sets of analytic spectra together are more reliable in analyzing and disentangling the RGW contributions from observational data [44, 45, 46].

The synchronous gauge has been often used, in which the decomposition of generic metric perturbations h_{ij} into the scalar, vector, and tensorial types is straightforward. For the scalar metric perturbations, this gauge is also more efficient in dealing with the adiabatic and isocurvature initial conditions, adequate for numerical computations [14, 15]. In comparison with the conformal Newtonian gauge [40], there are residual gauge freedoms in the synchronous gauge in the solution of scalar metric perturbations. By the restricted coordinate transformations [47, 48, 49], general solutions become rather involved for modes of arbitrary wavelengths. To implement analytical calculations, we work in the long wavelength approximation. Besides, a joining condition of the perturbation modes at the equality of radiation-matter will be chosen to ensure the continuity of the energy perturbations, not of the pressure.

In solving the Boltzmann's equation, One has to carry out the time-integrations for a_l^T and a_l^E from the RD epoch up to the present. The visibility function for the recombination process will appear in the integrations, and can be approximately fitted by the Gaussian type of functions [36, 37, 38, 50], in order to obtain the analytical expressions of a_l^T and a_l^E .

The organization of this paper is as follows. In Section 2, we introduce the convention of the decomposition of the scalar metric perturbations h_{ij} into two independent modes $h(\tau)$ and $\eta(\tau)$ in the flat Robertson-Walker metric. In Section 3, the Boltzmann's equation of the CMB radiation

field in the Basko-Polnarev's framework is formally solved in terms of two time-integrations for the temperature anisotropies $\alpha_k(\tau)$ and polarizations $\beta_k(\tau)$, respectively. The integrands consist of some combinations of the metric perturbations, the monopole α_0 , and the dipole α_1 of the temperature anisotropies as well. The fitting formula for the visibility function involved in the integrand is introduced. In Section 4, in the tight-coupling approximation, both α_0 and α_1 are solved in terms of the metric perturbations. In Section 5, the time-integrations are carried out, yielding the analytical expressions of $a_l^T(\tau)$ and $a_l^E(\tau)$, respectively. In Section 6, we will remove the gauge modes from the scalar metric perturbations for the RD and the MD eras, make a joining connection of the perturbations at the radiation-matter equality, and choose the proper initial conditions for the perturbations. In Section 7, we present the final analytical spectra C_l^{TT} , C_l^{TE} , and C_l^{EE} , and compare them with the numerical and the observed results. Several interesting properties of CMB anisotropies and polarization are revealed by the analytic spectra. Section 8 summarizes the main results and discusses possible future improvements. The Appendix provides the formulae that relate the multipole moments a_l^T and a_l^E to α_k and β_k , respectively. The unit with $\hbar = c = k_B = 1$ will be used.

2. Scalar Metric Perturbations in Synchronous Gauge

For a spatially flat ($k = 0$) Robertson-Walker (RW) space-time, the metric is

$$ds^2 = a^2(\tau)[-d\tau^2 + (\delta_{ij} + h_{ij})dx^i dx^j]. \quad (1)$$

where $a(\tau)$ is the scale factor as a function of the comoving time τ . The normalization of the scale factor is taken such that $a(\tau_0) = 2/H_0$ at the present time τ_0 , where H_0 is the Hubble constant. In our calculation, the RD and MD stages of the cosmic expansion are involved, for which the scale factor can be taken as the following form [43]:

$$a(\tau) = \frac{4}{H_0 \sqrt{1 + z_{eq}}} \tau, \quad \tau < \tau_2; \quad (2)$$

$$a(\tau) = \frac{2}{H_0} (\tau + \tau_2)^2, \quad \tau \geq \tau_2, \quad (3)$$

respectively, where $\tau_2 = 1/(2\sqrt{1 + z_{eq}}) \simeq 0.0085$ is the radiation-matter equality for $z_{eq} \simeq 3400$ [4], and $\tau_0 = 1 - \tau_2$. In this convention, the recombination time $\tau_d \simeq 0.0216$, corresponding to a redshift $z \sim 1100$. As will be seen in Section 3, the precise value of τ_d actually depends upon the baryon fraction Ω_b . To keep our analytical calculations simple, we do not include the current accelerating stage, which will bring some minor modifications to the CMB spectra. The metric perturbations in the synchronous gauge h_{ij} in Eq.(1) can be generally decomposed as

$$h_{ij} = \frac{1}{3} h \delta_{ij} + h_{ij}^{\parallel} + h_{ij}^{\perp} + h_{ij}^{\top}. \quad (4)$$

Here h_{ij}^\perp is the transverse ($\partial_i \partial_j h_{ij}^\perp = 0$), vector mode, and is usually neglected as it decays with the cosmic expansion. h_{ij}^\top is the transverse ($\partial_i h_{ij}^\top = 0$), tensorial mode, i.e., RWG. Its analytic solution and the analytical spectra $C_l^{XX'}$ induced by h_{ij}^\top have been studied before [22, 37, 38, 51]. We consider the remaining part, which is the scalar metric perturbations,

$$h_{ij} = \frac{1}{3} h \delta_{ij} + h_{ij}^\parallel, \quad (5)$$

where $h \equiv h_i^i$ is the trace part, and h_{ij}^\parallel is the traceless and longitudinal part, satisfying

$$\epsilon_{ijk} \partial_j \partial_l h_{lk}^\parallel = 0.$$

It can be expressed in terms of a scalar function,

$$h_{ij}^\parallel = \left(\partial_i \partial_j - \frac{1}{3} \delta_{ij} \nabla^2 \right) v. \quad (6)$$

Thus the density perturbations h_{ij} are described by two scalar functions, and can be written as a Fourier integration [43, 52]

$$h_{ij}(\mathbf{x}, \tau) = \int d^3 k e^{i \mathbf{k} \cdot \mathbf{x}} \left(\sum_{s=1,2} p_{ij}^s h_k^s(\tau) \right), \quad \mathbf{k} = k \vec{e}_k, \quad (7)$$

where $h_k^1(\tau)$ and $h_k^2(\tau)$ are the two scalar functions introduced, and

$$p_{ij}^1 = \vec{e}_{k_i} \vec{e}_{k_j}, \quad p_{ij}^2 = (\vec{e}_{k_i} \vec{e}_{k_j} - \frac{1}{3} \delta_{ij}) \quad (8)$$

are the two corresponding polarization tensors for the density perturbations. If we write

$$\overset{1}{h}_k(\tau) = h_k(\tau), \quad \overset{2}{h}_k(\tau) = 6\eta_k(\tau), \quad (9)$$

then $h_k(\tau)$ and $\eta_k(\tau)$ are the scalar modes used in Ref.[52]. If we write

$$\overset{1}{h}_k(\tau) = -H_{l k}(\tau) + 3H_k(\tau), \quad \overset{2}{h}_k(\tau) = -3H_k(\tau), \quad (10)$$

then H_k and $H_{l k}$ are identified as the scalar modes employed in Refs. [49, 43], where small letters h_k and $h_{l k}$ were used. The sets (h, η) in Eq.(9) is related to the set (H, H_l) in Eq.(10) as the following

$$H = -2\eta, \quad H_l = -(h + 6\eta), \quad (11)$$

where the sub-index k has been omitted in the following when no confusion arises.

An important property of density perturbations is that, a \mathbf{k} mode of h_{ij} in Eq.(5) is rotationally symmetric about the \mathbf{k} axis. Let the polar axis z be along $\hat{\mathbf{k}}$. The \mathbf{k} mode of the trace part $\frac{1}{3} h \delta_{ij}$ is isotropic in space, and the longitudinal part h_{ij}^\parallel has only the zz component. This is also reflected

by its polarizations $\overset{1}{p}_{ij}$ and $\overset{2}{p}_{ij}$ given in Eq.(8) that only depend on the vector $\hat{\mathbf{k}}$, independent of any vector perpendicular to \mathbf{k} . So the \mathbf{k} mode of h_{ij} is independent of the azimuthal angle ϕ . In contrast, a \mathbf{k} mode (plane wave) of GW h_{ij}^\top is transverse, with two components $h_{xx} = -h_{yy}$ and $h_{xy} = h_{yx}$. Therefore, h_{ij}^\top is not rotationally symmetric about the \mathbf{k} axis, and does depend on the azimuthal angle ϕ . Due to this difference, as we shall see later, the ϕ -independent density perturbation does not induce the magnetic type of polarization of CMB, whereas the ϕ -dependent GW does.

In order to calculate the evolution of CMB anisotropies and polarization, one needs the dynamic evolution of scalar perturbations $h(\tau)$ and $\eta(\tau)$ that enters the Boltzmann's equation of photons. However, in the synchronous gauge, the solution of $h(\tau)$ and $\eta(\tau)$ contain the residual gauge modes for both the RD and MD stages, which have to be dealt with later (in Section 6).

3. Boltzmann's equation in RW spacetime

The temperature field of CMB is not exactly isotropic, instead it has anisotropies, which are related to the metric perturbations h_{ij} via the Sachs-Wolf term. Moreover, the quadrupole component of the temperature anisotropies will be further induced by the linear polarizations via the Thomson scattering during the recombination. So the radiation field is described by the following column vector [43, 23, 24, 53, 54]

$$\vec{n} = \frac{1}{2\nu^3} \begin{pmatrix} I + Q \\ I - Q \\ -2U \end{pmatrix}, \quad (12)$$

where I is the intensity of radiation, and Q and U together describe the linear polarizations. The column \vec{n} can be split into two parts

$$\vec{n} = n^{(0)}\vec{u} + \vec{n}^{(1)} \quad \text{with} \quad \vec{u} \equiv \begin{pmatrix} 1 \\ 1 \\ 0 \end{pmatrix}, \quad (13)$$

where $n^{(0)}$ is the homogeneous, isotropic and unpolarized Planck spectrum in the expanding universe with frequency rescaled by the scale factor $\tilde{\nu} = \nu a(\tau)$, and $\vec{n}^{(1)} = \vec{n}^{(1)}(\tau, x^i, \nu, e^i)$ represents the temperature anisotropies and polarizations caused by the metric perturbation h_{ij} , and is a function of the conformal time τ , the comoving spatial coordinates x^i , the photon frequency ν , and the photon propagation direction $e^i = (\sin \theta \cos \phi, \sin \theta \sin \phi, \cos \theta)$.

Parallel to the Fourier expansion of h_{ij} in Eq.(7), $\vec{n}^{(1)}$ is also expanded into:

$$\vec{n}^{(1)}(\tau, x^i, \nu, e^i) = \int d^3k e^{i\mathbf{k}\cdot\mathbf{x}} \vec{n}_k^{(1)}(\tau, \nu, e^i).$$

For each Fourier component $\vec{n}_k^{(1)}(\tau, \nu, e^i)$, up to the first order of perturbations, the Boltzmann's equation is written as [43, 54]:

$$\left(\frac{\partial}{\partial \tau} + q(\tau) + ie^i k_i\right) \vec{n}_k^{(1)}(\tau, \nu, e^i) = \frac{f(\tilde{\nu})n^{(0)}(\tilde{\nu})}{2} \left(e^i e^j \sum_{s=1,2}^s \hat{p}_{ij} \frac{dh_k(\tau)}{d\tau} - q(\tau) e^i v_i \right) \vec{u} + \frac{q(\tau)}{4\pi} \int d\Omega' \hat{\mathbf{P}}(e^i; e'^j) \vec{n}_k^{(1)}(\tau, \nu, e'^j), \quad (14)$$

where the differential optical depth $q(\tau) = \sigma_T N_e(\tau) a(\tau)$ with σ_T being the Thomson cross section, and $N_e(\tau)$ being the comoving number density of free electrons, $f(\tilde{\nu}) = -\frac{\partial \ln n^{(0)}}{\partial \ln \tilde{\nu}}$, $e^i e^j \sum_{s=1,2}^s \hat{p}_{ij}$ and $\frac{d}{d\tau} h_k(\tau)$ being the Sachs-Wolfe term [16] reflecting the frequency variation due to h_{ij} , and v_i is the velocity of scattering electrons with respect to the chosen synchronous coordinate system. In the frame associated with the density waves with a wavevector $\vec{k}/k = (0, 0, 1)$ in \hat{z} direction, one has $e^i v_i = -i\mu v_b$ with $\mu = \cos \theta$ and v_b being the baryon (electron) velocity, $e^i e^j \hat{p}_{ij}^1 = \mu^2$, and $e^i e^j \hat{p}_{ij}^2 = (\mu^2 - 1/3)$, independent of the azimuthal angle ϕ . Thus, as is expected, the Sachs-Wolfe term is ϕ -independent, because the \mathbf{k} mode of density perturbation h_{ij} is ϕ -independent, as mentioned in Section 2. Then, the only term in Eq.(14) that might possibly depend on ϕ is the scattering term $\int d\Omega' \hat{\mathbf{P}}(e^i; e'^j) \vec{n}_k^{(1)}(\tau, \nu, e'^j)$, where the ϕ -dependent part of the Chandrasekhar matrix $\hat{\mathbf{P}}(e^i; e'^j)$ is only through $\sin(\phi' - \phi)$ and $\cos(\phi' - \phi)$ [53]. When one takes $\vec{n}_k^{(1)}$ to be independent of ϕ , the ϕ -dependent part of $\int_0^{2\pi} d\phi' \hat{\mathbf{P}}(e^i; e'^j)$ is vanishing due to $\int_0^{2\pi} d\phi' \sin(\phi' - \phi) = \int_0^{2\pi} d\phi' \cos(\phi' - \phi) = 0$. Therefore, in the case of density perturbations, it is consistent to take $\vec{n}_k^{(1)}$ independence of ϕ . This ϕ -independent property is the reason that the magnetic type polarization is not sourced by density perturbations (see Appendix). In contrast, for the case of GW, the term $e^i e^j \sum_{t=1,2}^t \hat{p}_{ij} \frac{dh_k(\tau)}{d\tau} \propto \cos 2\phi$, depending on ϕ . This ϕ -dependent property is also responsible for the magnetic type polarization generated by GW (see Appendix).

To further decompose Eq.(14), one can follow the treatment of Basko and Polnarev [23, 24, 54] and writes $\vec{n}_k^{(1)}$ in the following form:

$$\vec{n}_k^{(1)}(\tau, \nu, \mu) = \frac{f(\nu)n^{(0)}(\nu)}{2} \left[\alpha_k(\tau, \mu) \begin{pmatrix} 1 \\ 1 \\ 0 \end{pmatrix} + \beta_k(\tau, \mu) \begin{pmatrix} 1 \\ -1 \\ 0 \end{pmatrix} \right], \quad (15)$$

where α_k is the temperature anisotropies and β_k is the polarization. By comparing Eq.(12) and Eq.(15), it is seen that, for each wavenumber k , α_k is proportional to the anisotropic part of the intensity I ,

$$I(\tau, \mu) = \gamma \alpha_k(\tau, \mu) \quad (16)$$

with the factor $\gamma \equiv \nu^3 f(\nu) n^{(0)}(\nu)$, and $\beta_k(\mu)$ is related to the linear polarization Q itself

$$Q(\tau, \mu) = \gamma \beta_k(\tau, \mu). \quad (17)$$

Note that, by Thomson scattering of the unpolarized light at the last scattering, the Stokes parameter $U = 0$ for the \mathbf{k} mode of density perturbation. If the metric perturbation is GW, the form of $\vec{n}_k^{(1)}$ will be more complicated than Eq.(15), with all three Stokes parameters $I = I(\theta, \phi)$, $Q = Q(\theta, \phi)$, and $U = U(\theta, \phi) \neq 0$, depending on both angles (θ, ϕ) [23, 24, 36]. See the Appendix for the details.

Then Eq.(14) is converted into a set of two coupled first order differential equations for α_k and β_k [43, 54],

$$\left(\frac{\partial}{\partial\tau} + q(\tau) + ik\mu\right)\alpha_k = \frac{1}{2}\left(\frac{dH}{d\tau} - \mu^2\frac{dH_l}{d\tau}\right) + q(\tau)\left(\mathcal{I}_1(\tau) + i\mu v_b - \frac{1}{2}P_2(\mu)\mathcal{I}_2(\tau)\right), \quad (18)$$

$$\left(\frac{\partial}{\partial\tau} + q(\tau) + ik\mu\right)\beta_k = \frac{1}{2}q(\tau)(1 - P_2(\mu))\mathcal{I}_2(\tau), \quad (19)$$

where $P_2(\mu)$ is the second order Legendre function, and

$$\mathcal{I}_1(\tau) \equiv \frac{1}{2}\int_{-1}^1 d\mu\alpha_k(\tau, \mu), \quad (20)$$

$$\mathcal{I}_2(\tau) \equiv \frac{1}{2}\int_{-1}^1 d\mu[(1 - P_2(\mu))\beta_k(\tau, \mu) - P_2(\mu)\alpha_k(\tau, \mu)], \quad (21)$$

play a role of sources for α_k and β_k . On the right hand side of Eq.(18), $\frac{1}{2}(\frac{dH}{d\tau} - \mu^2\frac{dH_l}{d\tau})$ is the Sachs-Wolfe term, which has an counterpart in the case of RGW [36, 37, 38]. In contrast to the case of RGW, the second term on the right hand side of Eq.(18) is a new collision term, containing v_b , \mathcal{I}_1 , and \mathcal{I}_2 , which all contribute to the temperature anisotropies α_k . From Eq.(19) one sees that \mathcal{I}_2 enters the collision term and plays the role of the source for the polarization β_k . To solve the set of equations (18) and (19), one needs the quantities of $q(\tau)$, $H(\tau)$, $H_l(\tau)$, $v_b(\tau)$, \mathcal{I}_1 and \mathcal{I}_2 , which will be determined in Section 5 and Section 6.

Although formally similar to the case of RGW [36, 37, 38], Eqs.(18) and (19) are more complicated. There are residual gauge modes contained in the solutions of $H(\tau)$ and $H_l(\tau)$ for the RD and MD eras that have to be removed before one can actually calculate α_k and β_k . Also, the collision term $q(\tau)(\dots)$ on the right hand side of Eq.(18) is absent in the case of RGW, and needs some extra, proper treatments here.

We proceed to write down the formal solutions to Eqs.(18) and (19) as the following time integrations

$$\alpha_k(\tau, \mu) = \int_0^\tau d\tau' e^{-\kappa(\tau, \tau') - i\mu k(\tau - \tau')} \left[\frac{1}{2}\left(\frac{dH}{d\tau'} - \mu^2\frac{dH_l}{d\tau'}\right) + q(\tau')(\mathcal{I}_1(\tau') + i\mu v_b - \frac{1}{2}P_2(\mu)\mathcal{I}_2(\tau')) \right], \quad (22)$$

$$\beta_k(\tau, \mu) = \frac{1}{2}(1 - P_2(\mu)) \int_0^\tau d\tau' q(\tau') e^{-\kappa(\tau, \tau') - i\mu k(\tau - \tau')} \mathcal{I}_2(\tau'), \quad (23)$$

respectively, where

$$\kappa(\tau, \tau') \equiv \int_{\tau'}^{\tau} d\tau'' q(\tau'') = \kappa(\tau') - \kappa(\tau), \quad (24)$$

and the optical depth for the recombination

$$\kappa(\tau) \equiv \kappa(\tau_0, \tau) = \int_{\tau}^{\tau_0} d\tau' q(\tau') \quad (25)$$

from the present time τ_0 back to an earlier time τ , whose time derivative yield the differential optical depth

$$q(\tau) = -\dot{\kappa}(\tau) \equiv -\frac{d\kappa(\tau)}{d\tau}. \quad (26)$$

From $\kappa(\tau)$ and $q(\tau)$ follow the visibility function [40, 55, 56, 57, 58, 59, 60]

$$V(\tau) = \frac{d}{d\tau} e^{-\kappa(\tau)} = q(\tau) e^{-\kappa(\tau)}. \quad (27)$$

and the exponential function

$$e^{-\kappa(\tau)} = \int_{\tau_0}^{\tau} V(\tau) d\tau. \quad (28)$$

The quantities $q(\tau)$, $\kappa(\tau)$, $e^{-\kappa(\tau)}$, and $V(\tau)$ are equivalent in describing the recombination process. In principle, for a given cosmological model with a known $a(\tau)$, once the number density of free electrons $N_e(\tau)$ given explicitly for the detailed recombination process, one can calculate directly the differential optical depth $q(\tau)$, $\kappa(\tau)$, and $V(\tau)$ from their definitions [37, 38, 56]. The visibility function $V(\tau)$ has a statistical interpretation as the probability that a CMB photon we observe was last scattered at an earlier time τ , so that it satisfies the normalization condition

$$\int_0^{\tau_0} V(\tau) d\tau = 1. \quad (29)$$

Here we do not consider the reionization process [38], which would bring another term into the integrand in Eq.(29). The recombination process and the corresponding $V(\tau)$ depend on the matter fraction Ω_m and the baryon fraction Ω_b . As depicted in Fig.1, $V(\tau)$ is rather sharply distributed around the recombination time τ_d , and, among other things, its dependence upon the baryon fraction Ω_b is such that a greater Ω_b yields a slightly larger recombination time τ_d . In our context, by $\kappa(\tau_d) = 1$. According to [40], one has

$$\tau_d + \tau_2 \simeq 10^{-3/2} \Omega_b^{0.215/(16+1.8 \ln \Omega_b)}. \quad (30)$$

In practice, $V(\tau)$ is often be approximated by some fitting formulae [58, 40, 37, 38]. For the purpose of analytic calculations of CMB polarization, $V(\tau)$ was further simplified by a single Gaussian type of function [26, 35]

$$V(\tau) = V(\tau_d) \exp\left(-\frac{(\tau - \tau_d)^2}{2\Delta\tau_d^2}\right), \quad (31)$$

where $V(\tau_d) = (\sqrt{2\pi}\Delta\tau_d)^{-1}$ required by the normalization of Eq.(27), and $\Delta\tau_d$ is the half width and reflects the thickness of recombination. $\Delta\tau_d$ also depends on the baryon fraction Ω_b , and a larger Ω_b yields a slightly narrower $\Delta\tau_d$. It can be approximately fitted by

$$\Delta\tau_d \simeq 10^{-4}(8 - 2.33 \ln \Omega_b). \quad (32)$$

For the redshift thickness of the recombination $\Delta z \simeq 195 \pm 2$ by WMAP1 [4], the corresponding conforming time width is $2\Delta\tau_d \simeq 0.003$ for $\Omega_b = 0.045$. As adopted in the case of RGW [36, 37, 38], for a better approximation, $V(\tau)$ has also been fitted by two pieces of half Gaussian functions

$$V(\tau) = \begin{cases} V(\tau_d) \exp\left(-\frac{(\tau-\tau_d)^2}{2\Delta\tau_{d1}^2}\right), & (\tau \leq \tau_d), \\ V(\tau_d) \exp\left(-\frac{(\tau-\tau_d)^2}{2\Delta\tau_{d2}^2}\right), & (\tau > \tau_d), \end{cases} \quad (33)$$

where $\Delta\tau_{d1} = 0.0011$ and $\Delta\tau_{d2} = 0.0019$ for $\Omega_b = 0.045$ and $(\Delta\tau_{d1} + \Delta\tau_{d2})/2 = \Delta\tau_d$. It has been checked that the errors between Eq.(33) and the approximate formulae proposed in Refs. [40, 58] are very small, $< 4\%$ for $\tau > \tau_d$. Eq.(33) improves the description of visibility function by $\sim 10\%$ in accuracy over Eq.(31), and at the same time allows an analytical calculation of $C_l^{XX'}$.

Now back to $\alpha_k(\tau, \mu)$ and $\beta_k(\tau, \mu)$ in Eqs.(22) and (23). To get rid of their dependence of $\mu = \cos \theta$, one proceeds to expand them in terms of the Legendre functions:

$$\alpha_k(\tau, \mu) = \sum_l (-i)^l \alpha_l(\tau) P_l(\mu), \quad (34)$$

$$\beta_k(\tau, \mu) = \sum_l (-i)^l \beta_l(\tau) P_l(\mu), \quad (35)$$

with the multipole moments given by

$$\alpha_l(\tau) = i^l \frac{2l+1}{2} \int_{-1}^{+1} d\mu \alpha_k(\tau, \mu) P_l(\mu), \quad (36)$$

$$\beta_l(\tau) = i^l \frac{2l+1}{2} \int_{-1}^{+1} d\mu \beta_k(\tau, \mu) P_l(\mu), \quad (37)$$

where the following normalization condition has been used

$$\int_{-1}^1 dx P_l(x) P_{l'}(x) = \frac{2}{2l+1} \delta_{ll'}. \quad (38)$$

Inserting Eqs.(34) and (35) into Eqs.(20) and (21), carrying out the angular integration $\int d\mu$ there, and using the relation $(2l+1)xP_l(x) = (l+1)P_{l+1}(x) + lP_{l-1}(x)$, the sources \mathcal{I}_1 and \mathcal{I}_2 can be expressed in terms of the multipoles as the following:

$$\mathcal{I}_1(\tau) = \alpha_0(\tau), \quad (39)$$

$$\mathcal{I}_2(\tau) = \beta_0(\tau) + \frac{1}{5}\beta_2(\tau) + \frac{1}{5}\alpha_2(\tau). \quad (40)$$

In particular, Eq.(40) tells that the quadrupole α_2 of the temperature anisotropies enters \mathcal{I}_2 as a source for the polarization mode $\beta_l(\tau)$. In the following we will express $\mathcal{I}_1(\tau)$ and $\mathcal{I}_2(\tau)$ in terms of the scalar perturbations $h(\tau)$ and $\eta(\tau)$.

4. Determination of Integrands for $\alpha_k(\tau)$ and $\beta_k(\tau)$

The Boltzmann's equation (18) and (19) can be written as hierarchical sets of equations for the multipole moments α_l and β_l as the following.

For each l , multiplying both sides of Eq.(18) by $P_l(\mu)$ and integrating over $\frac{1}{2} \int_{-1}^1 d\mu$, one arrives at the hierarchical set of equations for α_l :

$$\dot{\alpha}_0 = -k\frac{1}{3}\alpha_1 + \frac{1}{3}\dot{h}, \quad (41)$$

$$\dot{\alpha}_1 = k(\alpha_0 - \frac{2}{5}\alpha_2) - q(\alpha_1 - v_b), \quad (42)$$

$$\dot{\alpha}_2 = k(\frac{2}{3}\alpha_1 - \frac{3}{7}\alpha_3) - \frac{2}{3}(\dot{h} + 6\dot{\eta}) - q(\tau)(\frac{9}{10}\alpha_2 - \frac{1}{2}\beta_0 - \frac{1}{10}\beta_2), \quad (43)$$

$$\dot{\alpha}_l = k(\frac{l}{2l-1}\alpha_{l-1} - \frac{l+1}{2l+3}\alpha_{l+1}) - q\alpha_l, \quad l \geq 3. \quad (44)$$

Note that the monopole $\alpha_0 = \delta T/T = \delta_\gamma/4$, where $\delta_\gamma = \delta\rho_\gamma/\rho_\gamma$ of the photon gas, and the dipole moment α_1 represents the velocity of photon gas. Eq.(41) shows that the metric perturbation $h(\tau)$ induces the generation of anisotropies α_0 . Similar treatments of Eq.(19) yield:

$$\dot{\beta}_0 = -k\frac{1}{3}\beta_1 + q(-\frac{1}{2}\beta_0 + \frac{1}{10}(\alpha_2 + \beta_2)), \quad (45)$$

$$\dot{\beta}_1 = k(\beta_0 - \frac{2}{5}\beta_2) - q\beta_1, \quad (46)$$

$$\dot{\beta}_2 = k(\frac{2}{3}\beta_1 - \frac{3}{7}\beta_3) + q(\tau)(\frac{1}{2}\beta_0 + \frac{1}{10}\alpha_2 - \frac{9}{10}\beta_2), \quad (47)$$

$$\dot{\beta}_l = k(\frac{l}{2l-1}\beta_{l-1} - \frac{l+1}{2l+3}\beta_{l+1}) - q\beta_l, \quad l \geq 3. \quad (48)$$

As Eq.(45) demonstrates, the quadrupole of temperature anisotropies α_2 is the major source for the leading order polarization β_0 via scattering. The above hierarchical sets, for both α and β , have infinite number of differential equations, and should be made closed in order to find their solutions. One takes the cutoff

$$\alpha_l = 0, \quad \beta_l = 0, \quad (l \geq 3), \quad (49)$$

which is justified for the long wave modes with $k\tau \ll 1$. Dropping the small quadrupole α_2 , Eq. (42) reduces to

$$\dot{\alpha}_1 = k\alpha_0 - q(\alpha_1 - v_b). \quad (50)$$

The term $-q(\alpha_1 - v_b)$ represents the momentum transfer from the baryon (electron) into the photon component. The quantity $1/q$ has the meaning of the mean free path of photons, and is a small parameter before the recombination. Before the recombination, photons and baryons are tightly coupled, and in the tight-coupling limit $1/q \rightarrow 0$, Eq. (50) implies $\alpha_1 = v_b$ so that photons and baryons behave like a coupled single fluid [59]. But, for a more accurate account for the difference between photons and baryons, one keeps up to the order of $1/q$. To deal with v_b , one needs to use the momentum conservation in Thomson scattering, i.e., the Euler equation for the electron velocity (See Eq.(66) in Ref. [52])

$$\dot{v}_b = -\frac{\dot{a}}{a}v_b + c_s^2 k^2 \delta_b + \frac{q}{R}(\alpha_1 - v_b), \quad (51)$$

where $R \equiv 3\rho_b/4\rho_\gamma$ is 3/4 times the baryon-photon ratio and, for a model $\Omega_b \sim 0.045$, can still be treated as $\ll 1$ during the recombination, and $c_s = 1/\sqrt{3(1+R)}$ is the sound speed of the photon gas. In the tight-coupling limit, the particle collision rate via Thomson scattering is much greater than the expansion rate, i.e., $q \gg \dot{a}/a$. So, in the long wavelength limit, Eq.(51) reduces to

$$\dot{v}_b \simeq \frac{q}{R}(\alpha_1 - v_b). \quad (52)$$

Now by combination of Eqs.(41), (50), and (52), one obtains the following second order differential equation of the monopole:

$$\ddot{\alpha}_0 + c_s^2 k^2 \alpha_0 = S(\tau) \quad (53)$$

with the source

$$S(\tau) \equiv \frac{1}{3}\ddot{h} = \ddot{H} - \frac{1}{3}\ddot{H}_l, \quad (54)$$

where the second equal sign follows by Eqs.(11). Note that c_s appearing in Eq.(53) is a function of time through the ratio R . At the level of our analytical calculation, R will be approximately treated as a constant, and its value will be taken at $z \sim 1100$ around the recombination. The general solution of Eq.(53) is given by the following simple form

$$\alpha_0(\tau) = B_1 \cos(p\tau) + B_2 \sin(p\tau) + \int_0^\tau \frac{S(\tau') \sin(p\tau - p\tau')}{p} d\tau', \quad (55)$$

where $p \equiv c_s k$, and B_1 and B_2 are constants, to be fixed by initial conditions. As we shall see later in Section 6, both B_1 and B_2 can be set to vanish. Once the scalar perturbation mode $h(\tau)$ is specified, the monopole $\alpha_0(\tau)$ follows from Eq.(55), and so does the source $\mathcal{I}_1(\tau)$ via Eq.(39). We remark that if the expansion term $-\frac{\dot{a}}{a}v_b$ in Eq.(51) was kept, Eq.(53) would be modified as the following

$$\ddot{\alpha}_0 + \frac{\dot{R}}{1+R}\dot{\alpha}_0 + c_s^2 k^2 \alpha_0 = \frac{\dot{R}}{1+R}\frac{1}{3}\dot{h} + S(\tau). \quad (56)$$

With R being a time-dependent function, this differential equation could also be solved, whose solution would differ only slightly from Eq.(55) on large scales under consideration ($l \lesssim 400$). In order to get full-analytical formulae, we use Eq.(55).

Once $\alpha_0(\tau)$ and $h(\tau)$ are known, the dipole α_1 follows immediately from Eq.(41),

$$\alpha_1(\tau) = \frac{3}{k}(-\dot{\alpha}_0 + \frac{1}{3}\dot{h}). \quad (57)$$

Let us calculate the source \mathcal{I}_2 for polarization in Eq.(40). It is interesting that a linear combination of Eqs.(43), (45), and (47), with higher order terms ($l \geq 3$) in perturbations being dropped, leads to the following differential equation

$$\dot{\mathcal{I}}_2 + \frac{3q}{10}\mathcal{I}_2 = M(\tau) \quad (58)$$

with

$$M(\tau) \equiv -\frac{2}{5}\dot{\alpha}_0(\tau) - \frac{4}{5}\dot{\eta}(\tau) = -\frac{2}{5}\dot{\alpha}_0 + \frac{2}{5}\dot{H}. \quad (59)$$

Eqs.(58) and (40), tell that $M(\tau)$ is the source of β_0 and of α_2 , simultaneously, and is expected to contribute equally to them as well. Eq.(58) has a formal solution

$$\mathcal{I}_2(\tau) = \int_0^\tau d\tau' M(\tau') e^{-\frac{3}{10}\kappa(\tau, \tau')} \quad (60)$$

with $\kappa(\tau, \tau')$ being defined in Eq.(24). As will be seen later, $M(\tau)$ is basically contributed by the gradient of the peculiar velocity of photon fluid, $k\alpha_1(\tau)$. When the perturbation mode $\eta(\tau)$ is specified, one calculates \mathcal{I}_2 from Eq.(60) straightforwardly. Having obtained \mathcal{I}_1 and \mathcal{I}_2 , one proceeds to perform the time integrations of the modes α_k and β_k .

5. Time Integrals for Temperature Anisotropies and Polarization

As demonstrated in Appendix, by projecting α_k and β_k on the basis $P_l(\mu)$ in Eqs.(140) and (141), one obtains the multipole moments a_l^T and a_l^E for the temperature anisotropies and the electric type of polarization respectively, which have been given by Eqs.(133) and (139) as the following

$$a_l^T = \int_0^{\tau_0} d\tau \left[\left(\dot{H} + \dot{H}_l \frac{d^2}{d\zeta^2} \right) e^{-\kappa(\tau)} + V(\tau) \left(\mathcal{I}_1 + v_b \frac{d}{d\zeta} - \frac{3}{4}\mathcal{I}_2 \left(1 + \frac{d^2}{d\zeta^2} \right) \right) \right] j_l(\zeta), \quad (61)$$

$$a_l^E = \frac{3}{4} \left(\frac{(l+2)!}{(l-2)!} \right)^{1/2} \int_0^{\tau_0} d\tau V(\tau) \mathcal{I}_2(\tau) \frac{j_l(\zeta)}{\zeta^2}, \quad (62)$$

where the variable $\zeta \equiv k(\tau_0 - \tau)$. These two time integrations have to be carried out.

First, we calculate a_l^E . Substituting \mathcal{I}_2 of Eq.(60) into Eq.(62) gives

$$a_l^E = \frac{3}{4} \left(\frac{(l+2)!}{(l-2)!} \right)^{1/2} \int_0^{\tau_0} d\tau V(\tau) \frac{j_l(\zeta)}{\zeta^2} \int_0^\tau d\tau' M(\tau') e^{-\frac{3}{10}\kappa(\tau') + \frac{3}{10}\kappa(\tau)}. \quad (63)$$

As we have seen, the visibility function $V(\tau)$, as an integrand, is narrowly peaked around the recombination time τ_d with a width $\Delta\tau_d$, so, for the τ -integration in Eq.(63), the integrand around τ_d only will have significant contributions. Moreover, in the τ' -integration the exponential factor $e^{-\frac{3}{10}\kappa(\tau')}$ behaves like a step function: $e^{-\frac{3}{10}\kappa(\tau')} \simeq 0$ for $\tau < \tau_d$, and $e^{-\frac{3}{10}\kappa(\tau')} \simeq 1$ for $\tau > \tau_d$. Thus, the integrand factor $M(\tau')$ can be approximately pulled out of the τ' -integration, leading to

$$a_l^E = \frac{3}{4} \left(\frac{(l+2)!}{(l-2)!} \right)^{1/2} \int_0^{\tau_0} d\tau V(\tau) \frac{j_l(\zeta)}{\zeta^2} M(\tau) \int_0^\tau e^{-\frac{3}{10}\kappa(\tau') + \frac{3}{10}\kappa(\tau)} d\tau'. \quad (64)$$

To perform the τ' -integration in Eq.(64), one introduces a variable $x \equiv \frac{\kappa(\tau')}{\kappa(\tau)}$ to replace the variable τ' [61, 38]. The corresponding limits of integration are $\tau' = \tau \rightarrow x = 1$ and $\tau' = 0 \rightarrow x = \infty$. Since $V(\tau)$ is peaked around τ_d with a width $\Delta\tau_d$, one can take $d\tau' \simeq -\frac{dx}{x} \Delta\tau_d$ as an approximation, valid over the period $\Delta\tau_d$ around the recombination. For a justification of this approximation, in Fig.2 we plot the optical depth $\kappa(\tau)$ as given in Ref.[40], which indeed behaves approximately as an exponential: $\kappa(\tau) \propto e^{-\tau/\Delta\tau_d}$ around τ_d . Then

$$a_l^E = \frac{3}{4} \left(\frac{(l+2)!}{(l-2)!} \right)^{1/2} \Delta\tau_d \int_0^{\tau_0} d\tau V(\tau) \frac{j_l(\zeta)}{\zeta^2} M(\tau) \int_1^\infty \frac{dx}{x} e^{-\frac{3}{10}\kappa(\tau)x + \frac{3}{10}\kappa(\tau)}. \quad (65)$$

$V(\tau)$ contains $e^{-\gamma(\tau-\tau_d)^2}$, and $j_l(\zeta)$ contains a mixture of oscillating modes $e^{ip\tau}$ and $e^{-ip\tau}$ with $p \propto k$. Using the formula of a form $\int_{-\infty}^\infty e^{-\gamma\tau^2} e^{ip\tau} d\tau = e^{-p^2/4\gamma} \int_{-\infty}^\infty e^{-\gamma\tau^2} d\tau$, the τ -integration is rendered approximately into

$$\int_0^{\tau_0} d\tau V(\tau) \frac{j_l(\zeta)}{\zeta^2} M(\tau) \approx \frac{j_l(\zeta_d)}{\zeta_d^2} M(\tau_d) D_E(k) \int_0^{\tau_0} d\tau V(\tau), \quad (66)$$

where

$$D_E(k) = 0.2(e^{-c_E(k\Delta\tau_1)^{b_E}} + e^{-c_E(k\Delta\tau_2)^{b_E}}) \quad (67)$$

is the Silk damping factor [62] for the polarization. It arises because the CMB photons diffuse through baryons and smaller scale fluctuations are smoothed, i.e., those modes of higher k are more effectively suppressed. Mathematically, it occurs as a sort of the Fourier transformation of $V(\tau)$ in Eq.(33). This is one of the advantages of our calculation in that the Silk damping factor arises naturally instead of adding by hand. c_E and b_E are two fitting parameters, and the values $c_E \sim 0.27$ and $b_E \sim 2.0$ yield an agreeing match with the numerical results [14, 15] over a range $l \lesssim 500$. The physical interpretation of the appearance of $D(k)$ associated with the recombination process has been given in Refs. [36, 37]. During the recombination around the time τ_d , the last scattering of CMB photons off baryons occur effectively only within a time interval $\sim \Delta\tau_d$. Putting it in terms of the spatial scale, the smoothing of density fluctuations by the associated diffusion through baryons occur effectively only on a scale of the thickness of the last scattering surface $\sim \Delta\tau_d$ (note that we use unit $c = 1$). Those modes, $e^{ik\tau}$ and $e^{-ik\tau}$, with wavelengths shorter than

$\sim \Delta\tau_d$ are effectively damped, whereas the long-wavelength modes are less damped. We remark that, as a fitting formula, $D_E(k)$ in Eq.(67) works only approximately, since other time-dependent factors in the integrand have been treated as constants. Besides, there are other processes [40, 63], which are significant on small scales, are not taken into account here. So the parameters c_E and b_E are introduced in Eq.(67) for adjustments. Among the two terms in Eq.(67), $D_E(k)$ is more sensitive to the term with a smaller time interval $\Delta\tau_1$.

The remaining double integration in Eq.(65) can be carried straightforwardly

$$\int_0^{\tau_0} d\tau V(\tau) \int_1^\infty \frac{dx}{x} e^{-\frac{3}{10}\kappa(\tau)x + \frac{3}{10}\kappa(\tau)} = \int_0^\infty d\kappa e^{-\frac{7}{10}\kappa} \int_1^\infty \frac{dx}{x} e^{-\frac{3}{10}\kappa x} = \frac{10}{7} \ln \frac{10}{3}, \quad (68)$$

whereby Eq.(27) has been used in the first equality. The above treatment of the integrations is similar to that in Refs.[36, 37, 38] for the case of RGW as the source. One arrives at the explicit, analytical formula of the multipole moment of polarization

$$a_l^E \simeq \frac{15}{14} \ln \frac{10}{3} \left(\frac{(l+2)!}{(l-2)!} \right)^{1/2} \frac{\Delta\tau_d}{k^2(\tau_0 - \tau_d)^2} M(\tau_d) D_E(k) j_l(k(\tau_0 - \tau_d)), \quad (69)$$

which depends upon the function $M(\tau_d)$ at the recombination time τ_d . As a marked feature, a_l^E contains explicitly the recombination width $\Delta\tau_d$, which arises from the τ' -integration in Eq.(64). Since $\Delta\tau_d$ is small, the amplitude of a_l^E will be consequently small, in comparison with a_l^T , whose dominant part does not contain this $\Delta\tau_d$ as will be seen later in this Section. Physically, the factor $M(\tau)$ represents the source of both the leading order polarization β_0 and the quadrupole temperature anisotropies α_2 , and contributes equally to them as well. As its time accumulated effect, the factor $\Delta\tau_d M(\tau_d)$ appears in a_l^E in Eq.(69) and in the last term of a_l^T in Eq.(78) as the quadrupole temperature anisotropies. During the course of time, the contribution of $M(\tau)$ is significant only around the recombination time τ_d with a width $\Delta\tau_d$. Note that the spherical Bessel functions $j_l(k(\tau_0 - \tau_d))$ in Eq.(69) is narrowly peaked around $k(\tau_0 - \tau_d) \simeq l$ for $l \gg 1$. In our notation $\tau_0 - \tau_d \sim 0.97$. So, for each given multipole l , the factor $j_l(k(\tau_0 - \tau_d))$ serves as a filter, selecting those modes with a wavenumber $k \sim l$ for a_l^E .

Next, we calculate a_l^T in Eq.(61). The first term in the integrand of Eq.(61) is the integrated Sachs-Wolfe (ISW) contribution, and contains the exponential factor $e^{-\kappa(\tau)}$, which can be roughly approximated by a step function [37, 38]:

$$e^{-\kappa(\tau)} = \begin{cases} 0, & \text{for } \tau < \tau_d, \\ 1, & \text{for } \tau_d \leq \tau \leq \tau_0. \end{cases} \quad (70)$$

So the ISW term is approximated by

$$\int_0^{\tau_0} d\tau \left(\dot{H} + \dot{H}_l \frac{d^2}{d\zeta^2} \right) e^{-\kappa(\tau)} j_l(\zeta) = \int_{\tau_d}^{\tau_0} d\tau \left(\dot{H} j_l(\zeta) + \dot{H}_l \frac{d^2}{d\zeta^2} j_l(\zeta) \right), \quad (71)$$

where the lower limit has also been replaced by τ_d . In the pertinent domain, $\dot{H}(\tau)$ and $\dot{H}_l(\tau)$ are comparable to each in magnitude, whereas in Eq.(71), the integrated value of $\frac{d^2}{d\zeta^2}j_l(\zeta)$ is two orders of magnitude smaller than that of $j_l(\zeta)$, so the term $\frac{d^2}{d\zeta^2}j_l(\zeta)$ in Eq.(71) can be neglected in the estimation. So the left-hand side of Eq.(71) reduces to

$$\int_{\tau_d}^{\tau_0} d\tau \dot{H} j_l(\zeta) \simeq (H(\tau_0) - H(\tau_d)) j_l(k\tau_0). \quad (72)$$

The second integration in Eq.(61) is

$$\int_0^{\tau_0} d\tau V(\tau) \left[\alpha_0 + \alpha_1 \frac{d}{d\zeta} - \frac{3}{4} \int_0^\tau e^{-\frac{3}{10}\kappa(\tau,\tau')} M(\tau') d\tau' \left(1 + \frac{d^2}{d\zeta^2} \right) \right] j_l(\zeta), \quad (73)$$

where we have substituted $\mathcal{I}_1 = \alpha_0$, $v_b = \alpha_1$ in the tight-coupling limit, and \mathcal{I}_2 as given in Eq.(60). The first two terms in Eq.(73) can be treated as before, yielding

$$\int_0^{\tau_0} d\tau V(\tau) \alpha_0(\tau) j_l(\zeta) \simeq \alpha_0(\tau_d) D_T(k) j_l(k(\tau_0 - \tau_d)), \quad (74)$$

$$\int_0^{\tau_0} d\tau V(\tau) \alpha_1(\tau) \frac{d}{d\zeta} j_l(\zeta) \simeq \alpha_1(\tau_d) D_T(k) \frac{d}{d\zeta} j_l(k(\tau_0 - \tau_d)), \quad (75)$$

where the damping factor for the temperature anisotropies is taken as

$$D_T(k) = \frac{1}{2} (e^{-c_T(k\Delta\tau_1)^{b_T}} + e^{-c_T(k\Delta\tau_2)^{b_T}}), \quad (76)$$

with c_T and b_T being two fitting parameters, and $c_T \sim 0.65$ and $b_T \sim 0.6$ yield a good match with numerical results by CAMB over a range $l \lesssim 500$. The last term in Eq.(73) is a double time integration and has the same structure as a_l^E in Eq.(63), and can be treated in the same way, yielding

$$\begin{aligned} & -\frac{3}{4} \int_0^{\tau_0} d\tau V(\tau) \left(1 + \frac{d^2}{d\zeta^2} \right) j_l(\zeta) \int_0^\tau e^{-\frac{3}{10}\kappa(\tau,\tau')} M(\tau') d\tau' \\ & \simeq -\frac{15}{14} \ln \frac{10}{3} \Delta\tau_d M(\tau_d) D_E(k) \left(1 + \frac{d^2}{d\zeta^2} \right) j_l(\zeta)|_{\zeta=k(\tau_0-\tau_d)}. \end{aligned} \quad (77)$$

Again, the term proportional to $\frac{d^2}{d\zeta^2}j_l(\zeta)$ can be neglect when calculating the power spectrum in Section 7. Putting these four pieces together, one arrives at the explicit, analytical formula of the multipole moment of temperature anisotropies

$$\begin{aligned} a_l^T & = \alpha_0(\tau_d) D_T(k) j_l(k(\tau_0 - \tau_d)) + \alpha_1(\tau_d) D_T(k) \frac{d}{d\zeta} j_l(k(\tau_0 - \tau_d)) \\ & + (H(\tau_0) - H(\tau_d)) j_l(k\tau_0) \\ & - \frac{15}{14} \ln \frac{10}{3} \Delta\tau_d M(\tau_d) D_E(k) \left(1 + \frac{d^2}{d\zeta^2} \right) j_l(\zeta)|_{\zeta=k(\tau_0-\tau_d)}. \end{aligned} \quad (78)$$

In the above expression, the α_0 term is dominant, the α_1 term is secondary, the ISW term is smaller than the α_1 term, and the last term containing the factor $\Delta\tau_d$ is smaller than the ISW term.

Note that the two major terms, α_0 and α_1 , in Eq.(78) do not contain $\Delta\tau_d$. This is because their corresponding integrations, Eqs.(74) and (75), are single time integrations, instead of double time integration. By comparison, the amplitude of a_l^T is expected to be higher than that of a_l^E . We note that the structure of a_l^T in Eq.(78) is similar to the parallel formula in the Newtonian gauge given in Ref.[40], which did not have the last term $\propto \Delta\tau_d M(\tau_d)$. The relative contributions of the four terms in Eq.(78) will be demonstrated in Fig.6.

To completely determine a_l^T in Eq.(69) and a_l^E in Eq.(78), one still needs α_0 , α_1 , $M(\tau)$ in Eqs.(55), (57), and (59), respectively, which all depend upon the scalar perturbations $h(\tau)$ and $\eta(\tau)$. In the following we will solve for $h(\tau)$ and $\eta(\tau)$.

6. Determination of scalar perturbations

The unperturbed spacetime background are described by the Friedmann equations:

$$\left(\frac{\dot{a}}{a}\right)^2 = \frac{8\pi}{3}Ga^2\bar{\rho}, \quad (79)$$

$$\frac{\ddot{a}}{a} = -\frac{4\pi}{3}Ga^2(\bar{\rho} + 3\bar{P}), \quad (80)$$

where $\bar{\rho}$ and \bar{P} are the mean energy density and pressure. The Einstein equations for the scalar perturbations in synchronous gauge are the following [49, 52]

$$k^2\eta - \frac{1}{2}\frac{\dot{a}}{a}\dot{h} = 4\pi Ga^2\delta T_0^0, \quad (81)$$

$$k^2\dot{\eta} = 4\pi Ga^2 ik^j \delta T_j^0, \quad (82)$$

$$\ddot{h} + 2\frac{\dot{a}}{a}\dot{h} - 2k^2\eta = -8\pi Ga^2\delta T_i^i, \quad (83)$$

$$\ddot{h} + 6\ddot{\eta} + 2\frac{\dot{a}}{a}(\dot{h} + 6\dot{\eta}) - 2k^2\eta = -24\pi Ga^2(\bar{\rho} + \bar{P})\sigma, \quad (84)$$

where σ represents the anisotropic stress, $\delta T_0^0 = -\bar{\rho}\delta$ is the perturbed energy density, $\delta T_i^i = 3\delta P$ is the perturbed pressure, and $\frac{\delta P}{\delta\rho} = c_s^2$, where the sound speed $c_s \simeq \frac{1}{3}$ in RD era and $c_s \simeq 0$ in MD era.

First, let us do for the RD era. We are concerned with the long wave modes with $k\tau \ll 1$, and the solutions of the set of Eqs.(81)-(84) for h and η are [47, 48, 49, 52]

$$h = A + B(k\tau)^{-2} + C(k\tau)^2 + D(k\tau), \quad (85)$$

$$\eta = 2C + \frac{3}{4}D(k\tau)^{-1}. \quad (86)$$

All the coefficients A through D actually depend on the comoving wavenumber k , which has been skipped hereafter for notational simplicity. The two terms proportional to A and B are gauge modes, which will be dropped, and two physical modes are proportional to C and D .

$$h = C(k\tau)^2 + D(k\tau). \quad (87)$$

Among these two modes, the mode $(k\tau)^2$ grows faster and is dominant at late times, and the mode $(k\tau)$ is less important, which was neglected in the treatment of Ref.[52] and was taken to be small in Ref.[49]. In principle, the two coefficients C and D should be determined by either the inflationary or the reheating era that precedes the RD era. To avoid further complication from the preceding eras, we shall treat D as a small parameter proportional to C . For simplicity of analytical calculations, we do not include the modifications due to cosmic neutrinos, which will bring higher order terms $(k\tau)^2$ to η during the RD era [52]. Let us examine the long wave approximation during the RD era. At the radiation-matter equality τ_2 the comoving sound horizon is $\sim c_s\tau_2$. Those k -modes with $1/k > c_s\tau_2$ can be taken as the long wave modes during the RD era. In our notation with the comoving time τ specified from Eq.(1) through Eq.(3), this is equivalent to $k \lesssim 210$ (0.025 Mpc^{-1}). For wave number greater than this, a more elaborated treatment of the perturbations during the RD would be desired than presented here.

For the MD era, the solution of the metric perturbations are given by [47, 48, 49, 52]

$$h = J + (k\tau)^2 E + \frac{1}{(k\tau)} F + \frac{1}{(k\tau)^3} G, \quad (88)$$

$$\eta = 5E - \frac{1}{(k\tau)^3} F, \quad (89)$$

where the constant J is a gauge mode corresponding to a transformation of the spatial coordinates, i.e., a rescaling of the scale factor $a(\tau)$, and can be dropped. As has been known [47], for $h(\tau)$ in Eq.(88), the linear combination $\frac{2}{(k\tau)} + \frac{1}{(k\tau)^3}$ is another gauge mode, which is dominated by $\frac{1}{(k\tau)^3}$ for $k\tau \ll 1$ (long wavelengths or early time), and by $\frac{1}{(k\tau)}$ for $k\tau \gg 1$ (short wavelengths or late time). In our context, we aim at the large angular temperature anisotropies and polarization of CMB. So we are concerned with the long wavelength perturbations around the radiation-matter equality τ_2 and the recombination time τ_d . Thus the G term is taken as the dominant gauge mode. To keep our analytical calculation simple, we drop the G term. In fact, the G term is the time-translation-invariant solution and can be gauged away by a restricted coordinate transformation within in the synchronous gauge [48]. Other discussions on gauge modes are given in Refs. [47, 49]. The term proportional to E in Eq.(88) grows with time and is the primary portion of the physical mode. Thus, for the MD era, one has

$$h = (k\tau)^2 E + \frac{1}{(k\tau)} F, \quad (90)$$

$$\eta = 5E - \frac{1}{(k\tau)^3} F. \quad (91)$$

From these specifications, the source $S(\tau)$ in Eq.(54) reduces to

$$S(\tau) = \frac{2k^2}{3} C, \quad \text{for RD}, \quad (92)$$

$$S(\tau) = \frac{2k^2}{3}E + \frac{2}{3k\tau^3}F, \quad \text{for MD.} \quad (93)$$

Now we need to make a proper connection of the perturbations for the RD and MD eras at the radiation-matter equality $\tau = \tau_2$. We remark that the energy density perturbation δ is continuous in the transition from RD to MD era. But the pressure P is not required to be so, as $P > 0$ during RD, and $P = 0$ during MD. By the perturbed Einstein equation Eq.(81) for δ , one finds that the combination $k^2\eta - \frac{1}{2}\frac{\dot{a}}{a}\dot{h}$ is required to be continuous at $\tau = \tau_2$. Since $\dot{a}(\tau)$ is continuous as prescribed in Eqs.(2) and (3), \dot{h} and η are required to be continuous, leading to

$$2k^2\tau_2 C + kD = 2k^2\tau E - \frac{F}{k\tau_2^2}, \quad (94)$$

$$2C + \frac{3}{4k\tau_2}D = 5E - \frac{1}{(k\tau_2)^3}F. \quad (95)$$

From these two algebraic equations, one solves for E and F in terms of C and D .

$$E = -\frac{D}{12k\tau_2}, \quad (96)$$

$$F = -(k\tau_2)^3 \left(2C + \frac{7D}{6k\tau_2} \right). \quad (97)$$

The coefficient D is a small parameter that needs to be fixed. We take the coefficient D to be smaller than C by a factor $(k\tau_2)$ in the long wavelength limit $k\tau \ll 1$, so that $D \sim (k\tau_2)C$. Specifically, in the following analytical calculations, we take

$$D = -\frac{24}{5}(k\tau_2)C, \quad (98)$$

though other possible choices may also be justified as long as D is subdominant to C in the long wavelength limit. Substituting Eq.(98) into the above yields

$$E = \frac{2}{5}C, \quad F = \frac{18}{5}(k\tau_2)^3C. \quad (99)$$

One can check that, in the RD, as well as in MD era, if we transform the perturbations h and η in synchronous gauge back to the ϕ and ψ in Newtonian gauge [40], the results are consistent with each other. Fig. 4 shows the continuous joining of the perturbation modes $h(\tau)$ and $\eta(\tau)$ at τ_2 , and Fig. 5 shows the continuous joining of the modes $H(\tau)$ and $H_l(\tau)$. As one can check, the functions \ddot{h} and $\dot{\eta}$ are not continuous at $\tau = \tau_2$ by our joining condition.

To fix the initial condition, we need to specify the k -dependent coefficient C . According to the inflationary models of the early universe, the primordial scalar perturbations were generated with a nearly scale-invariant spectrum with a spectral index $n_s \sim 1$ [64]. In our notation this corresponds to $C \propto k^{\frac{1}{2}(n_s-3)}$. For inflationary models proposed so far, the most uncertain quantity

is the amplitude of the spectrum. In practice, this can be fixed by cosmological observations, say, the WMAP result. One writes the curvature perturbation spectrum

$$\Delta_R^2(k) = \Delta_R^2(k_0) \left(\frac{k}{k_0} \right)^{n_s - 1 + \frac{1}{2}\alpha_s \ln(k/k_0)}, \quad (100)$$

where the physical pivot wavenumber $k_0 = 0.002 \text{Mpc}^{-1}$, $\Delta_R^2(k_0)$ is the normalization at k_0 . WMAP5 [7] gives $\Delta_R^2(k_0) = (2.41 \pm 0.11) \times 10^{-9}$, WMAP5+BAO+SN Mean [9] gives $\Delta_R^2(k_0) = (2.445 \pm 0.096) \times 10^{-9}$. Besides the scalar spectral index n_s , we include a possible scalar running spectral index α_s in the spectrum [31, 32]. The fitted value of n_s is much affected by the presence of α_s and the RGW component, and by additional combination with SN Ia and BAO data as well. In absence of α_s and the RGW, WMAP5 gives $n_s = 0.963_{-0.015}^{+0.014}$ [7], WMAP5 +SN Ia+BAO gives $n_s = 0.960_{-0.013}^{+0.014}$ [7], and WMAP7 gives $n_s = 0.963 \pm 0.012$ [9]. When α_s is allowed, WMAP5 gives $n_s = 1.087_{-0.073}^{+0.072}$ and $\alpha_s = -0.050 \pm 0.034$ with a better determination of the third acoustic peak [9], WMAP5+BAO+SN has given $n_s = 1.089_{-0.068}^{+0.070}$ and $\alpha_s = -0.053_{-0.028}^{+0.027}$ [7, 9]. More recent WMAP7+ACBAR+QUaD gives $n_s = 1.041_{-0.046}^{+0.045}$ and $\alpha_s = -0.041_{-0.023}^{+0.022}$ [8, 9]. When RGW is also allowed [34], WMAP7+Tensor gives $n_s = 1.076 \pm 0.065$, $\alpha_s = -0.048 \pm 0.029$, $r < 0.49$ [9]. In the slow-roll scalar inflationary models, n_s and α_s can be calculated from the inflationary potential and its derivatives [31, 32]. For generality, we will treat n_s and α_s as parameters. Eq.(100) corresponds to

$$C = C_0 \left(\frac{k}{k_C} \right)^{\frac{1}{2}(n_s - 3) + \frac{1}{4}\alpha_s \ln(k/k_0)}, \quad (101)$$

where the normalization $C_0 \sim 204$. The physical pivot wavenumber k_0 corresponds to a comoving wavenumber $k_C = k_0 a(\tau_0) \simeq 17.1$ for the Hubble parameter $H_0 = 70.1 \text{ km s}^{-1} \text{ Mpc}^{-1}$ [9].

In fixing the initial condition for α_0 at $k\tau \ll 1$ during the RD era, the coefficients B_1 and B_2 in Eq.(55) have to be specified. In the tight-coupling approximation, $k\alpha_1$ in Eqs.(41) can be neglected, yielding $\alpha_0 = h/3$ for $k\tau \ll 1$. By comparison, in the limit $k\tau \rightarrow 0$, h behaves as in Eq.(87), so the term $B_1 \cos(p\tau)$ in α_0 should be vanishing, leading to $B_1 = 0$. The $B_2 \sin(p\tau)$ term in Eq.(55) represents the isocurvature mode of initial perturbations. A stringent constraint has been given by WMAP5 on the isocurvature contribution with the isocurvature/adiabatic ratio $\alpha_{-1} < 0.015$ at 95% CL [7, 38]. For simplicity, we can choose the coefficient $B_2 = 0$. Then the monopole $\alpha_0(\tau)$ in Eq.(55) reduces to the integration

$$\alpha_0(\tau) = \int_0^{\tau_2} \frac{S(\tau') \sin(p\tau - p\tau')}{p} d\tau' + \int_{\tau_2}^{\tau} \frac{S(\tau') \sin(p\tau - p\tau')}{p} d\tau', \quad (102)$$

Using Eqs.(92), (93), (99) into the above yields the monopole

$$\begin{aligned} \alpha_0(\tau) &= 2C(1+R) \left[\frac{3}{5} \cos(p\tau - p\tau_2) - \cos p\tau + \frac{2}{5} \right] \\ &+ C(1+R) \frac{36}{5} \int_{\tau_2}^{\tau} \frac{1}{k^3 \tau'^3} \sin(p\tau - p\tau') d(p\tau'). \end{aligned} \quad (103)$$

From Eq.(57) and Eq.(90) follows the dipole

$$\begin{aligned}
\alpha_1(\tau) &= 2C\sqrt{3(1+R)} \left[\frac{3}{5} \sin(p\tau - p\tau_2) - \sin(p\tau) \right] \\
&\quad - C\frac{36}{5}\sqrt{3(1+R)} \int_{\tau_2}^{\tau} \left(\frac{\tau_2}{\tau'}\right)^3 \cos(p\tau - p\tau') d(p\tau') \\
&\quad + C\frac{4}{5}(k\tau) - C\frac{18}{5}\left(\frac{\tau_2}{\tau}\right)^2(k\tau_2).
\end{aligned} \tag{104}$$

By the definition in Eq.(59), we take time derivatives of $\alpha_0(\tau)$ and $\eta(\tau)$ in Eq.(103) and Eq.(89), respectively, and arrive at

$$\begin{aligned}
M(\tau) &= -\frac{4}{5}C(1+R) \left[-\frac{3}{5}p \sin(p\tau - p\tau_2) + p \sin p\tau \right] \\
&\quad - \frac{72}{25}C(1+R) \int_{\tau_2}^{\tau} \frac{\tau_2^3 p}{\tau'^3} \cos(p\tau - p\tau') d(p\tau') - C\frac{216}{25} \frac{\tau_2^3}{\tau^4}
\end{aligned} \tag{105}$$

for the MD era. We have checked that, in this final expression, $M(\tau)$ is dominated by the first two terms coming from $-2\dot{\alpha}_0(\tau)/5$, whereas the last term $-C\frac{216}{25}\frac{\tau_2^3}{\tau^4}$ coming from $-4\dot{\eta}(\tau)/5$ is comparatively small by more one order of magnitude. It is important to notice that, due to time differentiation, $M(\tau)$ contains the functions like $\sin(p\tau - p\tau_2)$, whereas $\alpha_0(\tau) \propto \cos(p\tau - p\tau_2) + \dots$. This fact will lead to the character of the present CMB that the peaks of the polarization $C_l^{EE} \propto |a_l^E|^2 \propto |\sin(p\tau_d - p\tau_2)|^2 + \dots$ and of the temperature anisotropies $C_l^{TT} \propto |a_l^T|^2 \propto |\cos(p\tau_d - p\tau_2)|^2 + \dots$ appear alternatingly.

Using Eqs.(11), (90), (91), and (99), the time derivatives of the scalar modes, \dot{H} and \dot{H}_l during MD, are given by

$$\dot{H}(\tau) = C\frac{108}{5} \frac{\tau_2^3}{\tau^4}, \tag{106}$$

$$\dot{H}_l(\tau) = -\frac{2}{5}C \left(2k^2\tau - 9k^2\frac{\tau_2^3}{\tau^2} + 162\frac{\tau_2^3}{\tau^4} \right). \tag{107}$$

So $\dot{H}(\tau)$ and $\dot{H}_l(\tau)$ are comparable to each in magnitude around the recombination.

7. The analytical spectra

Given the multipole moments a_l^E in Eq.(69) and a_l^T in Eq.(78), the spectra C_l^{TT} , C_l^{TE} , and C_l^{EE} are calculated as the following integrations over the wavenumber k [43]

$$C_l^{TT} = \int |a_l^T(k)|^2 k dk, \tag{108}$$

$$C_l^{TE} = \int a_l^T(k) a_l^E(k) k dk, \tag{109}$$

$$C_l^{EE} = \int |a_l^E(k)|^2 k dk. \tag{110}$$

The resulting spectra are explained in the following graphs.

Fig. 3 demonstrates the relative contributions by each term to C_l^{TT} . Over the relevant range $l \lesssim 500$, the contribution by ISW is rather flat as a function of l , and its amplitude is at most $\sim 10\%$ that of the α_1 term. The last term in Eq.(78) contains the factor $\Delta\tau_d M(\tau_d)$ given by setting $\tau = \tau_d$ in Eq.(105), and its contribution to a_l^T is even smaller than the ISW term, with two low bumps at $l \sim 130$ and at $l \sim 350$. The smallness of this term is due to the extra small factor $\Delta\tau_d \sim 0.003$. Thus, the major features of a_l^T in Eq.(78) are largely contributed by $\alpha_0(\tau_d)$ and $\alpha_1(\tau_d)$, whereas the quadrupole part of a_l^T contains the factor $\Delta\tau_d M(\tau_d)$, similar to the polarization a_l^E in Eq.(69). This also tells that the polarization a_l^E is smaller than the temperature anisotropies a_l^T in amplitude.

In Fig.6 we plot these analytical spectra $l(l+1)C_l^{TT}$, $l(l+1)C_l^{TE}$, $l(l+1)C_l^{EE}$ for $n_s = 0.96$, $\alpha_s = 0$, and the baryon fraction $\Omega_b = 0.045$. For comparison, the numerical result from CAMB [15] and the observed result from WMAP5 [7] are also given. For a more realistic case, one would have to also include the analytical $C_l^{XX'}$ by RGW [36, 37, 38] at a tensor/scalar ratio r to form the complete calculated $C_l^{XX'}$. We leave that for future studies. Fig.7 shows that the overall profiles of the analytical spectra agree well with the numerical and the observed on large angular scales with $l \lesssim 500$. This range covers the first primary peak of C_l^{TT} and the first two primary peaks of C_l^{EE} and of C_l^{TE} . Only around $l \simeq 310$ where the second primary peak of C_l^{TE} is located, the analytical C_l^{TE} deviates by $\sim 18\%$ higher in amplitude from the numerical one. For smaller angular scales, the analytical results deviate considerably from the numerical ones. This has been expected since our calculation is based upon the long wavelength approximation valid only for large angular scales. From Fig.6, we see that the first two peaks of C_l^{TT} occur at $l \sim 200$ and $l \sim 500$, while those of C_l^{EE} occur at $l \sim 100$ and $l \sim 400$. This alternating occurrence of the peak locations of C_l^{EE} and C_l^{TE} has been anticipated. (See the discussion below Eq.(105). Based on the analytic results, one can estimate the span of the two adjacent peaks of C_l^{EE} in l - space, which corresponds to that of $|\sin(c_s k(\tau_d - \tau_2))|^2$ in k - space. Since $j_l(k(\tau_0 - \tau_d))$ is significantly contributive only around $k(\tau_0 - \tau_d) \sim l$ for $l \gg 1$, it plays a role of a filter and selects those $k(\tau_0 - \tau_d) \sim l$ part of the integrand to contribute to the integration $\int dk$ over k . Qualitatively, the span Δk of two adjacent peaks of $|\sin(c_s k(\tau_d - \tau_2))|^2$ is given by a relation $\pi = c_s \Delta k(\tau_d - \tau_2)$. Then the span of the two adjacent peaks of C_l^{EE} in l - space is $\Delta l \sim \Delta k(\tau_0 - \tau_d) \sim 370$. The same Δl holds also for C_l^{TT} . This is roughly what is seen in Fig.7. (See also Ref.[65]).

In Fig.7, we sketch the profile of $l(l+1)C_l^{EE}$ as a function of l , which, notably, has two bumps, one at $l \sim 100$, and another at $l \sim 400$. In order to interpret the origin of these two bumps, we also sketch the main factor $D_E(k)M(\tau_d)/[k(\tau_0 - \tau_d)]^2$ of a_l^E in Eq.(69) as a function of k . By the projection of $j_l(k(\tau_0 - \tau_d))$, the square of $D_E(k)M(\tau_d)/[k(\tau_0 - \tau_d)]^2$ around $k \sim l$, aside some

factor, is basically C_l^{EE} around l . Since $D_E(k)M(\tau_d)/[k(\tau_0 - \tau_d)]^2$ has two bumps, around $k \sim 100$ and $k \sim 400$, they give rise to the two bumps of C_l^{EE} .

Fig.8 shows the first two peaks of the squared time derivative $k|\dot{\alpha}_0(\tau)|^2$. Below Eq.(105) we have mentioned that $-2\dot{\alpha}_0(\tau)/5$ is the dominant term of $M(\tau)$. Thus, it is the time derivative $\dot{\alpha}_0(\tau)$ that essentially determines the characteristic profile of C_l^{EE} , including the peak locations. The two peaks of $|\dot{\alpha}_0(\tau)|^2$ consequently gives rise to the first two peaks of C_l^{EE} , the first one actually being very low so that it is only a low bump.

Fig.9 shows the dependence of $C_l^{XX'}$ upon the scalar spectral index n_s . The pivot point $k_0 = 0.002\text{Mpc}^{-1}$ corresponds to $l \sim 12$. As is seen, a greater value of n_s yields a higher amplitude of $C_l^{XX'}$ for $l > 12$. This is expected from the initial amplitude C given in Eq.(101), which gets larger for a greater n_s in the range $k \geq k_{0C}$. The effect is most obvious around the primary peaks.

Fig.10 shows the dependence of $C_l^{XX'}$ upon the scalar running spectral index α_s . A greater α_s yields a higher amplitude of $C_l^{XX'}$ as is expected from Eq.(101) in the range $k \geq k_{0C}$. Comparing Fig.9 with Fig.10 reveals that there is a certain degree of degeneracy between the indices n_s and α_s as two major cosmological parameters. This degeneracy has demonstrated itself in fitting the observational data of WMAP [6, 7, 8, 9]. Therefore, given the accuracy of current observational data of $C_l^{XX'}$, it is not easy to distinguish the fine details of the inflation potentials.

Fig.11 shows the dependence of $C_l^{XX'}$ upon the baryon fraction Ω_b , in the amplitudes and the locations of peaks and troughs. As is seen, a greater value of Ω_b yields higher amplitudes of C_l^{TT} (also see Refs. [40],[55], [56], [58]) and C_l^{TE} , but a lower amplitude of C_l^{EE} . This can be understood as follows. Eqs.(103) and (104) show that a greater Ω_b corresponds to a greater R and gives higher amplitudes of α_0 and α_1 , hence a higher amplitude of a_l^T in Eq.(78) and of C_l^{TT} . On the other hand, a_l^E in Eq.(69) is proportional to the recombination width $\Delta\tau_d$, which is smaller for a greater value of Ω_b as fitted by Eq.(32). Thus C_l^{EE} has a lower amplitude for a greater Ω_b . As for the cross spectrum C_l^{TE} , the Ω_b -dependence of its amplitude is the outcome of these two competing factors. Since greater n_s and Ω_b both tend to enhance the amplitudes of the spectra C_l^{TT} and C_l^{TE} , there is also a degeneracy between n_s and Ω_b in regards to C_l^{TT} and C_l^{TE} . Nevertheless, for the spectrum C_l^{EE} , greater n_s and Ω_b have just opposite effects on its amplitude. This feature will help to break the degeneracy. Fig.11 also shows that a greater Ω_b shifts the locations of peaks and troughs of $C_l^{XX'}$ to larger l (smaller angles). This is because a greater Ω_b leads to a lower sound speed c_s of photon gas, so at a fixed frequency the corresponding wavelength is suppressed [66]. By the analytic results, this is evident from the oscillating factors $\sin(c_s k \tau_0)$ and $\cos(c_s k \tau_0)$ contained in a_l^T and a_l^E , whose peak locations are stretched to a larger wavenumber k (i.e., larger l via the projection of $j_l(k(\tau_0 - \tau_d))$) for a smaller c_s .

Fig.12 shows that a longer recombination process (a greater $\Delta\tau_d$) yields a higher amplitude of

polarization. This property has been obvious since the analytic expression in Eq.(69) tells $a_l^E \propto \Delta\tau_d$. Fig.12 also shows that a longer recombination process brings more damping of C_l^{EE} on small scales. This is because a_l^E in Eq.(69) contains the damping factor $D_E(k) \propto e^{-c_E(k\Delta\tau_d)^2}$. Similarly, this feature also is shared by C_l^{TT} , as the damping factor $D_E(k) \propto e^{-c_T(k\Delta\tau_d)^2}$ appears in the major term of a_l^T in Eq.(78).

Fig.13 shows that a longer $\Delta\tau_d$ yields higher peaks as well as lower troughs of C_l^{TE} . Moreover, a longer $\Delta\tau_d$ slightly shifts the peaks and troughs to larger scales and causes more damping on smaller scales. These features are helpful to probe $\Delta\tau_d$, as long as current and future CMB observational data are accurate enough. However, as an approximation, this analytic result also has its limitation, since the recombination history has been primarily represented by only two parameters: the recombination time τ_d and recombination width $\Delta\tau_d$ as an integrated effect. Two different recombination histories via different differential optical depth $q(\tau)$ would lead to the same amplitudes of bumps and troughs, as long as they have same τ_d and $\Delta\tau_d$.

Fig.14 shows that a late recombination (greater τ_d) shifts the peaks and troughs of the polarization C_l^{EE} to larger angular scales. The property also holds for C_l^{TT} and C_l^{TE} . This can be explained by the appearance of the function $j_l(k(\tau_0 - \tau_d))$ as a factor in the analytic expressions of a_l^T and a_l^E .

Fig.15 shows the ratios of the analytic spectra to the numerical spectra, $C_l^{TT}(a)/C_l^{TT}(n)$, and $C_l^{EE}(a)/C_l^{EE}(n)$. The ratios are seen to be centered around 1 for $l \leq 500$, showing a reasonable agreement between the analytic and numeric on large angular scales.

8. Conclusion and Discussions

In this paper, we have presented an analytical calculation of CMB anisotropies and polarization generated by scalar metric perturbations in the synchronous gauge, resulting in the explicit, analytic expressions of the multipole moments a_l^T in Eq.(78) and a_l^E in Eq.(69), and, thus, of all the analytical spectra C_l^{TT} , C_l^{EE} , and C_l^{TE} . This has been implemented primarily through an approximation treatment of time-integrations over the recombination process, a technique used before for the case with RGW as the generating source [36, 37, 38]. We have also dealt with the removal of the residual gauge modes and the joining condition at the equality of radiation-matter of the scalar perturbations. Several approximations have been used, such as the long wavelength approximation for scalar perturbations during the RD era, tight-coupling approximation for the photons during the recombination process.

These results are new and have significantly extended the earlier preliminary works. The analytic expressions of polarization a_l^E and the related spectra C_l^{EE} , and C_l^{TE} are what have not been addressed in Ref.[42]. Besides, our analytic expression a_l^T fulfils what was not completed in Ref.[43],

and, to a great extent, improves what was given in Ref.[42], as our expression a_l^T contains the separate contributions of monopole, dipole, quadrupole, and Sachs-Wolfe terms.

Our analytic calculation shows that the polarization a_l^E is generated mainly by the quadrupole of temperature anisotropies α_2 via scattering. Besides, a_l^E and of α_2 are simultaneously generated by the combination $M(\tau_d)$, so that the resulting a_l^E and α_2 have a similar structure and both are smaller than the total temperature anisotropies a_l^T .

Furthermore, the analytic expressions of a_l^E and a_l^T demonstrate explicitly that the peaks of the polarization C_l^{EE} and of the temperature anisotropies C_l^{TT} in l - space appear alternatingly. These help to understand the important features of $C_l^{XX'}$.

As the major advantage of analytic expressions, a_l^T and a_l^E explicitly show the dependance upon the scalar perturbations, initial amplitude C_0 , primordial spectrum index n_s , baryon fraction Ω_b , damping factor $D(k)$, recombination width $\Delta\tau_d$, and the recombination time τ_d . These properties are transparent in analytic expressions, but might not be directly obvious in the numerical code itself. For instance, the dependencies upon $\Delta\tau_d$ tell that a longer recombination process yields a higher amplitude of polarization since $a_l^E \propto \Delta\tau_d$, and brings more damping of a_l^T and a_l^E on small scales through $D_E(k)$, $D_T(k)$. The dependencies upon τ_d tell that a late recombination shifts the peaks and troughs of spectra $C_l^{XX'}$ to larger angular scales.

The spectra C_l^{TT} , C_l^{TE} and C_l^{EE} agree with the results of the numerical codes on large angular scales $l \lesssim 500$, covering the first two peaks and troughs of $C_l^{XX'}$. On smaller scales, the analytical spectra deviate considerably from the numerical ones, as is expected for the long wavelength approximations. Serving as a complement to the numerical studies, the preliminary analytical calculations efficiently promote the analysis of effects upon $C_l^{XX'}$ by various physical processes, and improve our understanding the important features of the observed CMB.

Based upon the framework presented in this paper, several points can be further improved for more accurate spectra $C_l^{XX'}$. Some of them are listed as the following. One can extend the analytical calculation to smaller scales [67]. For the solutions of perturbations h and η , Eqs.(85) and (86), one may include higher order terms in $k\tau$. Consistent with this, one could do a finer treatment of the baryon component before the recombination, including the time dependence of the ratio $R(\tau)$ as in Eq.(56). One could also try to include the modifications from the relativistic neutrino component during the RD era. Finer examinations can be made on the initial condition during the RD era. For instance, alternative forms could be tried for the slowly growing mode D other than that in Eq.(98), and possible allowances could be tested for initial isocurvature perturbations besides the adiabatic ones. Further examinations on the gauge modes for smaller scales could be made during the MD era. Very importantly, one should include the reionization occurred around a redshift $z \sim 11$, a process secondary only to the recombination. This will

definitely bring about modifications of $C_l^{XX'}$ on large angular scales $l \sim 5$ [38]. Finally, to extract possible signals of RGW from observations, one should separate the contribution of RGW with various ratio r from scalar perturbations in the total spectra $C_l^{XX'}$, which can be done within the framework in synchronous gauge by using the results in this paper and our previous work on RGW.

Appendix: The multipole moments for radiation field

On a 2-dimensional unit sphere with a metric

$$d\sigma^2 = g_{ab}dx^a dx^b = d\theta^2 + \sin^2 \theta d\phi^2, \quad (111)$$

a general radiation field is usually characterized by the following 2×2 polarization tensor [53, 29, 43],

$$P_{ab} = \frac{1}{2} \begin{pmatrix} I + Q & -(U - iV) \sin \theta \\ -(U + iV) \sin \theta & (I - Q) \sin^2 \theta \end{pmatrix} \quad (112)$$

with the four Stokes parameters (I, Q, U, V) , where I is the intensity of radiation, Q and U describe the linear polarization, and V is the circular polarization. In the case of CMB, the Thomson scattering during the recombination does not generate the circular polarization [53], so we set $V = 0$. Note that I is a scalar on the 2-dim sphere under the transformation of θ and ϕ , but Q and U transform among themselves. To deal with this problem, several formulations have been proposed, such as the total angular momentum method using the spin-weighted spherical harmonic functions [68], and the spin raising and lowering operator method [28, 29]. These two treatments are essentially equivalent, and the latter will be adopted in the following. The tensor in Eq.(112) consists of two parts:

$$P_{ab} = \frac{1}{2} I g_{ab} + P_{ab}^{STF},$$

where $\frac{1}{2} I g_{ab}$ for the temperature anisotropies is of scalar nature, and P_{ab}^{STF} for the polarization is the symmetric trace-free (STF):

$$P_{ab}^{STF} = \frac{1}{2} \begin{pmatrix} Q & -U \sin \theta \\ -U \sin \theta & -Q \sin^2 \theta \end{pmatrix}, \quad (113)$$

from which one can construct two linear independent, invariant quantities involving its second order covariant derivatives [43]:

$$E(\theta, \phi) = -2(P_{ab}^{STF})^{;a;b}, \quad B(\theta, \phi) = -2(P_{ab}^{STF})^{;b;d} \epsilon_d^a, \quad (114)$$

where

$$\epsilon_{ab} = \begin{pmatrix} 0 & -\sin \theta \\ \sin \theta & 0 \end{pmatrix} \quad (115)$$

is a completely antisymmetric pseudo-tensor. E is a scalar on the 2-sphere and B is a pseudo-scalar. It is revealing to write $P_a \equiv (P_{ab}^{STF})^{;b}$. Then $E = P_a^{;a}$ is a divergence of P_a , and $B = P_{a;b}\epsilon^{ab}$ is a curl of P_a . In this regard, E is referred to as the “electric” polarization, and B as the “magnetic” polarization. As can be checked, by directly calculating the covariant derivatives on the 2-sphere, one has [29, 28]

$$E = -\frac{1}{2}[\bar{\partial}^2(Q + iU) + \partial^2(Q - iU)], \quad (116)$$

$$B = \frac{i}{2}[\bar{\partial}^2(Q + iU) - \partial^2(Q - iU)], \quad (117)$$

where ∂^2 is the raising operator acting twice, and $\bar{\partial}^2$ is the lowering operator acting twice,

$$\partial^2(Q - iU)(\mu, \phi) = (-\partial_\mu - \frac{-i\partial_\phi}{1 - \mu^2})^2[(1 - \mu^2)(Q - iU)(\mu, \phi)], \quad (118)$$

$$\bar{\partial}^2(Q + iU)(\mu, \phi) = (-\partial_\mu + \frac{-i\partial_\phi}{1 - \mu^2})^2[(1 - \mu^2)(Q + iU)(\mu, \phi)], \quad (119)$$

where $\mu = \cos\theta$.

Since I , E , and B are scalars on the 2-sphere, they can be expanded in terms of the spherical harmonics $Y_{lm}(\theta, \phi)$ as a complete and orthonormal basis [43]:

$$I(\theta, \phi) = \sum_{l=0}^{\infty} \sum_{m=-l}^l a_{lm}^I Y_{lm}(\theta, \phi), \quad (120)$$

$$E(\theta, \phi) = \sum_{l=2}^{\infty} \sum_{m=-l}^l \left[\frac{(l+2)!}{(l-2)!} \right]^{\frac{1}{2}} a_{lm}^E Y_{lm}(\theta, \phi), \quad (121)$$

$$B(\theta, \phi) = \sum_{l=2}^{\infty} \sum_{m=-l}^l \left[\frac{(l+2)!}{(l-2)!} \right]^{\frac{1}{2}} a_{lm}^B Y_{lm}(\theta, \phi). \quad (122)$$

For technical simplicity, one can choose the coordinate with the polar axis $\hat{\mathbf{z}}$ pointing along the wave vector \mathbf{k} of the scalar perturbation mode: $\mathbf{k} \parallel \hat{\mathbf{z}}$. Let an unpolarized incident light have an intensity I' scattered on a charge. Using the differential Thomson scattering cross-section $\frac{d\sigma}{d\Omega} = \frac{3\sigma_T}{8\pi} |\epsilon' \cdot \epsilon|$, with ϵ' and ϵ being the polarization of incident and outgoing light, respectively, one obtains [27] $I = \frac{3\sigma_T}{16\pi}(\theta)I'(1 + \cos^2\theta)$, $Q = \frac{3\sigma_T}{16\pi}(\theta)I' \sin^2\theta$, and $U = 0$ for the outgoing wave, where θ is the angle between the incident and outgoing directions. The result does not depend on the azimuthal angle ϕ . As a corollary, in an azimuthal symmetric configuration, Thomson scattering of an unpolarized light yields

$$I = I(\theta), \quad Q = Q(\theta), \quad U = 0. \quad (123)$$

for the outgoing wave. This is just the situation with a \mathbf{k} -mode of density perturbations at the last scattering. As explained in Section 2, The \mathbf{k} -mode of density perturbation is azimuthal symmetric

about the \mathbf{k} axis. At the last scattering, the incident light is unpolarized. Therefore, in Eq.(15) we only need I and Q for a \mathbf{k} mode of the density perturbations [27, 28, 29].

Since Q only depends on θ , so that $\bar{\partial}^2 Q = \partial^2 Q = \partial_\mu^2[(1 - \mu^2)Q(\mu)]$, resulting

$$E = -\partial_\mu^2[(1 - \mu^2)Q(\mu)], \quad (124)$$

$$B = 0, \quad (125)$$

i.e., the scalar metric perturbations generate no polarization of magnetic type [28]. Another more geometric way to see why $B = 0$ and $E \neq 0$ is to use the definitions in Eq.(114). Since $U = 0$ for a \mathbf{k} -mode of density perturbation, the polarization matrix in Eq.(113) reduces to

$$P_{ab}^{STF} = \frac{1}{2} \begin{pmatrix} Q & 0 \\ 0 & -Q \sin^2 \theta \end{pmatrix}, \quad (126)$$

and, a direct calculation yields

$$E = -Q_{,\theta\theta} - \frac{\cos \theta}{\sin \theta} Q_{,\theta}, \quad (127)$$

$$B = \frac{2}{\sin \theta} Q_{,\theta\phi} + \frac{2 \cos \theta}{\sin^2 \theta} Q_{,\phi}. \quad (128)$$

This tell us that the magnetic type of polarization B essentially involves the derivative of Q with respect to ϕ , and is a measure of asymmetry of polarization field under the rotation about the \mathbf{k} axis. Since Q is independent of ϕ , one has $B = 0$.

It is interesting to compare with the case GW, where the rotational symmetry is lost for the \mathbf{k} mode of GW, and the outgoing light after Thomson scattering would be a general linear polarized one, with all three Stokes parameters $I = I(\theta, \phi)$, $Q = Q(\theta, \phi)$, and $U = U(\theta, \phi) \neq 0$, depending on θ as well as ϕ [23, 24, 36], and resulting in $E \neq 0$ and $B \neq 0$. This distinguished feature of non-vanishing magnetic type of polarization of CMB can be served as a possible channel to detect gravitational waves.

The multipole moments a_{lm}^T of temperature anisotropies and a_{lm}^E of the electric type of polarization are given by

$$a_{lm}^T(k) = 2\pi \int_{-1}^1 d\mu Y_{lm}^*(\mu) I(\tau, \mu), \quad (129)$$

$$a_{lm}^E(k) = 2\pi \left[\frac{(l-2)!}{(l+2)!} \right]^{\frac{1}{2}} \int_{-1}^1 d\mu Y_{lm}^*(\mu) E(\mu). \quad (130)$$

Both a_l^T and a_l^E are observables on the sky. Since I and E are now functions of θ only, one can set the magnetic index $m = 0$ in the above expressions and uses the replacements $Y_{l0}(\theta) = \sqrt{\frac{2l+1}{4\pi}} P_l(\mu)$ and $a_{lm}^T \rightarrow a_{l0}^T$ and $a_{lm}^E \rightarrow a_{l0}^E$.

Firstly, we calculate the multipole moments a_{l0}^T at the present time τ_0 . From Eq.(129), using Eq.(16) and Eq.(22), one has

$$\begin{aligned} a_{l0}^T(k) &= 2\pi\gamma\sqrt{\frac{2l+1}{4\pi}} \int_{-1}^1 d\mu P_l(\mu) \alpha_k(\tau_0, \mu) \\ &= 2\pi\gamma\sqrt{\frac{2l+1}{4\pi}} \int_{-1}^1 d\mu P_l(\mu) \int_0^{\tau_0} d\tau e^{-\kappa(\tau_0, \tau) - i\mu k(\tau_0 - \tau)} \left[\frac{dH}{d\tau} - \mu^2 \frac{dH_l}{d\tau} + q(\mathcal{I}_1 + i\mu v_b - \frac{1}{2}P_2(\mu)\mathcal{I}_2) \right]. \end{aligned}$$

Making use of the relation

$$\int_{-1}^1 d\mu P_l(\mu) e^{-i\mu x} = 2(-i)^l j_l(x), \quad (131)$$

the above expression of a_{l0}^T is reduced to

$$a_{l0}^T(k) = \gamma(-i)^l \sqrt{4\pi(2l+1)} a_l^T(k), \quad (132)$$

where

$$a_l^T(k) = \int_0^{\tau_0} d\tau \left[e^{-\kappa(\tau)} \left(\frac{dH}{d\tau} + \frac{dH_l}{d\tau} \frac{d^2}{d\zeta^2} \right) + V(\tau) \left(\mathcal{I}_1 - v_b \frac{d}{d\zeta} - \frac{3}{4} \mathcal{I}_2 \left(1 + \frac{d^2}{d\zeta^2} \right) \right) \right] j_l(\zeta), \quad (133)$$

with the variable $\zeta \equiv k(\tau_0 - \tau)$.

Next, we calculate the multipole moments a_{l0}^E at the present time τ_0 .

$$a_{l0}^E(k) = 2\pi \left[\frac{(l-2)!}{(l+2)!} \right]^{\frac{1}{2}} \sqrt{\frac{2l+1}{4\pi}} \int_{-1}^1 d\mu P_l(\mu) E(\mu). \quad (134)$$

By Eq.(17) and Eq.(124), one has

$$E(\mu) = -\gamma \partial_\mu^2 [(1 - \mu^2) \beta_k(\mu)]. \quad (135)$$

Substituting the expression β_k of Eq.(23) into Eq.(135) yields

$$\begin{aligned} E(\mu) &= -\gamma \frac{3}{4} \int_0^{\tau_0} d\tau V(\tau) \mathcal{I}_2(\tau) \partial_\mu^2 [(1 - \mu^2)^2 e^{-i\zeta\mu}] \\ &= \gamma \frac{3}{4} \int_0^{\tau_0} d\tau V(\tau) \mathcal{I}_2(\tau) (1 + \partial_\zeta^2)^2 (\zeta^2 e^{-i\zeta\mu}). \end{aligned} \quad (136)$$

Substituting Eq.(136) into Eq.(134) and using Eq.(131), one has

$$\begin{aligned} a_{l0}^E(k) &= \gamma 2\pi \sqrt{\frac{2l+1}{4\pi}} \frac{3}{4} \left[\frac{(l-2)!}{(l+2)!} \right]^{\frac{1}{2}} \int_0^{\tau_0} d\tau \int_{-1}^1 d\mu P_l(\mu) V(\tau) \mathcal{I}_2(\tau) (1 + \partial_\zeta^2)^2 (\zeta^2 e^{-i\zeta\mu}) \\ &= \gamma(-i)^l \sqrt{4\pi(2l+1)} \frac{3}{4} \left[\frac{(l+2)!}{(l-2)!} \right]^{\frac{1}{2}} \int_0^{\tau_0} d\tau V(\tau) \mathcal{I}_2(\tau) (1 + \partial_\zeta^2)^2 (\zeta^2 j_l(\zeta)). \end{aligned} \quad (137)$$

Using the relation for the spherical-Bessel functions

$$j_l''(x) + 2 \frac{j_l'(x)}{x} + \left[1 - \frac{l(l+1)}{x^2} \right] j_l(x) = 0$$

to replace $j_l''(\zeta)$, the term $(1 + \partial_\zeta^2)^2(\zeta^2 j_l(\zeta))$ in Eq.(137), one obtains

$$a_{l0}^E(k) = \gamma(-i)^l \sqrt{4\pi(2l+1)} a_l^E(k), \quad (138)$$

where

$$a_l^E(k) = \frac{3}{4} \left[\frac{(l+2)!}{(l-2)!} \right]^{\frac{1}{2}} \int_0^{\tau_0} d\tau V(\tau) \mathcal{I}_2(\tau) \frac{j_l(\zeta)}{\zeta^2}. \quad (139)$$

One can check that a_l^T and a_l^E in Eqs.(133) and (139) are essentially α_k and β_k projected on the basis $P_l(\mu)$, respectively:

$$a_l^T(k) = i^l \frac{1}{2} \int_{-1}^1 d\mu P_l \cdot \alpha_k(\tau, \mu), \quad (140)$$

$$a_l^E(k) = i^l \frac{1}{2} \int_{-1}^1 d\mu P_l \cdot \beta_k(\tau, \mu). \quad (141)$$

The main result of the Appendix is the expressions of a_l^T in Eq.(133) and a_l^E in Eq.(139), which have been used in Section 5.

ACKNOWLEDGMENT: Z. Cai has been partially supported by National Science Fund for Fostering Talents in Basic Science (J0630319), and Z. Cai would like to thank Prof. Li-Zhi Fang for his encouragements and thank Dr. Xiaohui Fan for partial supports. Y. Zhang's research work is supported by the CNSF No.11073018, SRFDP, and CAS.

References

- [1] P. de Bernadis, *et al.*, Nature **404**, 995 (2000);
P.D. Mauskopf, *et al.*, Astrophys. J. **536** (2000) L59;
A. Melchiorri, *et al.*, Astrophys. J. **536** (2000) L63;
A.E. Lange, *et al.*, Phys. Rev. D **63** 042001 (2001);
C.B. Netterfield, *et al.*, Astrophys. J. **571**, 604 (2002);
J. E. Ruhl, *et al.*, Astrophys. J. **599**, 786 (2003);
C. J. MacTavish, *et al.*, Astrophys. J. **647**, 799 (2006);
T.E. Montroy, *et al.*, Astrophys. J. **647**, 813 (2006);
W.C. Jones, *et al.*, Astrophys. J. **647**, 823 (2006);
F. Piacentini, *et al.*, Astrophys. J. **647**, 833 (2006).
- [2] S. Hanany, *et al.*, Astrophys. J. **545**, L5 (2000);
A. Balbi, *et al.*, Astrophys. J. **545**, L1 (2000);
R. Stompor, *et al.*, Astrophys. J. **561**, L7 (2001);
A.H. Jaffe, *et al.*, New Astron. Rev. **47**, 727 (2003);

- [3] E. M. Leitch, *et al.*, *Nature* **420**, 763 (2002);
 J. M. Kovac, *et al.*, *Nature* **420**, 772 (2002);
 N. W. Halverson, *et al.*, *Astrophys. J.* **568**, 38 (2002);
 C. Pryke, *et al.*, *Astrophys. J.* **568**, 46 (2002);
 E. M. Leitch, *et al.* *Astrophys. J.* **624**, 10 (2005).
- [4] C.L.Bennett, *et al.*, *Astrophys. J. Suppl. Ser.* **148**, 1 (2003);
 G. Hinshaw, *et al.*, *Astrophys. J. Suppl. Ser.* **148**, 63 (2003);
 A. Kogut, *et al.*, *Astrophys. J. Suppl. Ser.* **148**, 161 (2003);
 D. N. Spergel, *et al.*, *Astrophys. J. Suppl. Ser.* **148**, 175 (2003).
 D. Page, *et al.*, *Astrophys. J. Suppl. Ser.* **148**, 233 (2003);
 M.R. Nolta, *et al.*, *Astrophys. J.* **608**, 10 (2004).
- [5] H. V. Peiris, *et al.*, *Astrophys. J. Suppl. Ser.* **148**, 213 (2003).
- [6] G. Hinshaw, *et al.*, *Astrophys. J. Suppl. Ser.* **170**, 288 (2007);
 L. Page, *et al.*, *Astrophys. J. Suppl. Ser.* **170**, 335 (2007);
 D.N. Spergel, *et al.*, *Astrophys. J. Suppl. Ser.* **170**, 377 (2007).
- [7] G. Hinshaw, *et al.*, *Astrophys. J. Suppl. Ser.* **180**, 225 (2009);
 M. R. Nolta, *et al.*, *Astrophys. J. Suppl. Ser.* **180**, 296 (2009);
 J. Dunkley, *et al.*, *Astrophys. J. Suppl. Ser.* **180**, 306 (2009).
- [8] D. Larson *et al.*, *Astrophys. J. Suppl. Ser.* **192**, 16, (2011);
 N. Jarosik, *et al.*, arXiv:1001.4744;
- [9] E. Komatsu, *et al.*, *Astrophys. J. Suppl. Ser.* **180** 330 (2009); *Astrophys. J. Suppl. Ser.* **192**
 18 (2011).
- [10] A. Benoit, *et al.*, *Astron. Astrophys.* **399**, L19 (2003); *Astron. Astrophys.* **399**, L25 (2003);
 M. Tristram, *et al.*, *Astron. Astrophys.* **436**, 785 (2005).
- [11] A. C. S. Readhead, *et al.*, *Science*, **306**, 836 (2004);
 J. L. Sievers, *et al.*, *Astrophys. J.* **591**, 599 (2003) ;
 T. J. Pearson, *et al.*, *Astrophys. J.* **591** 556, (2003).
- [12] P. Ade, *et al.*, *Astrophys. J.* **674**:22-28, (2008);
 C. Pryke, *et al.*, *Astrophys. J.* **692**, 1247 (2009);
 P. G. Castro, *et al.*, *Astrophys. J.* **701**, 857 (2009);
 M. L. Brown, *et al.*, *Astrophys. J.* **705**, 978(2009);
 S. Gupta , *et al.*, *Astrophys. J.* **716**, 1040 (2010).
- [13] H. C. Chiang, *et al.*, *Astrophys. J.* **711** 1123 (2010).
- [14] U. Seljak and M. Zaldarriaga, *Astrophys. J.* **469**, 437 (1996);
 M. Zaldarriaga, U. Seljak, E. Bertschinger, *Astrophys. J.* **494**, 491 (1998);
 M. Zaldarriaga and U. Seljak, *Astrophys. J.* **129**, 431 (2000).
 The cmbfast Online Tool can be available at
http://lambda.gsfc.nasa.gov/toolbox/tb_cmbfast_form.cfm

- [15] A. Lewis, A. Challinor and A. Lasenby, *Astrophys. J.* **538**, 473 (2000).
The CAMB Online Tool can be available at
http://lambda.gsfc.nasa.gov/toolbox/tb_camb_form.cfm
- [16] R.K. Sachs and A.M. Wolfe, *Astrophys. J.* **147**, 73 (1967).
- [17] J.M. Bardeen, *Phys. Rev. D* **22**, 1882 (1980).
- [18] H. Kodama and M. Sasaki, *Prog. Theor. Phys. Supp.* **78**,1 (1984).
- [19] V.F.Mukhanov, H.A.Feldman, and R.H.Brandenberger, *Phys. Rep.* **215** (1992) 203.
- [20] L. P. Grishchuk, *Sov. Phys. JETP* **40**, 409 (1975); *Ann. N. Y. Acad.Sci.* **302** 439 (1977);
Class.Quant.Grav. **14** 1445 (1997);
in "*General Relativity and John Archibald Wheeler*", P.151, Ciufolini and Mastzner (Eds),
(Springer, 2010), arXiv:gr-qc/0707.3319;
in "*Gyros, Clocks, Interferometers...: Testing Relativistic Gravity in Space*", P.167, Lam-
merzahl, Everitt, and Hehl (Eds), (Springer, 2001), arXiv:gr-qc/0002035;.
- [21] L.H. Ford and L. Parker, *Phys. Rev. D* **16**, 1601 (1977).
A. A. Starobinsky, *JEPT Lett.* **30**, 682 (1979); *Sov. Astron. Lett.* **11** (1985) 133;
V. A. Rubakov, M.Sazhin, and A.Veryaskin, *Phys. Lett. B* **115**, 189 (1982);
R. Fabbri and M. D. Pollock, *Phys. Lett. B* **125** (1983) 445;
L. Abbott and M. Wise, *Nuc. Phys. B* **237** (1984) 226;
B. Allen, *Phys. Rev. D* **37**, 2078 (1988);
V. Sahni, *Phys. Rev. D* **42**, 453 (1990).
- [22] Y. Zhang, *et al.*, *Class. Quant. Grav.* **22**, 1383 (2005); *Chin. Phys. Lett.* **22**, 1817 (2005);
Class. Quant. Grav. **23**, 3783 (2006).
- [23] M.M. Basko and A.G. Polnarev, *Mon. Not. R. Astron. Soc.*, **191**, 207 (1980); *Sov.Astron.*
24, 268 (1984).
- [24] A.G. Polnarev, *Sov.Astron.* **29**, 607 (1985).
- [25] R.G. Crittenden, D. Coulson, and N. G. Turok, *Phys. Rev. D* **52**, 5402 (1995).
- [26] M. Zaldarriaga and D. D.Harari, *Phys. Rev. D* **52**, 3276 (1995).
- [27] A. Kosowsky, *Annal. Phys.* **246**, 49 (1996).
- [28] M. Zaldarriaga and U. Seljak, *Phys. Rev. D* **55**, 1830 (1997).
- [29] M. Kamionkowski, A. Kosowsky, A. Stebbins, *Phys. Rev. D* **55**, 7368 (1997).
- [30] B. Keating, P. Timbie, A. Polnarev, J. Steinberger, *Astrophys.J.* **495** 580 (1998).
- [31] A.R. Liddle and D. Lyth, *Phys. Lett. B* **291**, 391 (1992);
A. R. Liddle and M.S. Turner, *Phys. Rev. D* **50**, 758 (1994);
A.R. Liddle and D.H. Lyth, *Cosmological Inflation and Large-Scale Structure*, (Cambridge
University Press, 2000).
- [32] A. Kosowsky and M.S. Turner, *Phys. Rev. D* **52**, 1739 (1995).
- [33] LIGO Collaboration and VIRGO Collaboration, *Nature (London)* **460**, 990 (2009).

- [34] M.L. Tong , Y. Zhang, Phys. Rev. D**80**, 084022 (2009);
Y. Zhang, M. L. Tong, and Z. W. Fu, Phys. Rev. D**81** Rapid Communication, 101501 (2010).
- [35] J.R.Pritchard and M.Kamionkowski, Ann. Phys. (N.Y.) **318** 2 (2005).
- [36] W. Zhao and Y. Zhang, Phys. Rev. D**74**, 083006 (2006).
- [37] T.Y. Xia and Y. Zhang, Phys. Rev. D**78**, 123005 (2008);
Y. Zhang, *et al.*, Int. J. Mod. Phys. D Vol **17**, 1105 (2008).
- [38] T.Y. Xia and Y. Zhang, Phys. Rev. D**79**, 083002 (2009).
- [39] A. Challinor, A. Lasenby, Astrophys.J.**513**, 1 (1999).
- [40] W. Hu and N.Sugiyama, Astrophys.J. **444** 489 (1995); Phys. Rev. D **51** 2599 (1995); Astro-
phys. J. **471** 542 (1996).
- [41] W. Hu, Sugiyama N., and J. Silk, Nature **386**, 37 (1997).
- [42] S. Weinberg, Phys. Rev. D**64**, 123511 (2001); Phys.Rev. D**64** (2001) 123512.
- [43] D. Baskaran, L. P. Grishchuk, A. G. Polnarev, Phys. Rev. D **74**, 083008 (2006).
- [44] A. G. Polnarev, N. J. Miller, and B. G. Keating, Mon. Not. R. Astron. Soc., **386**, 1053 (2008);
N. J. Miller, B. G. Keating, and A. G. Polnarev, Adv. Astron. Astrophys.(09), 309024 (2009).
- [45] W. Zhao, D. Baskaran, L. P. Grishchuk, Phys. Rev. D **79**, 023002 (2009); Phys. Rev. D **80**,
083005 (2009); Phys. Rev. D **82**, 043003 (2010);
W. Zhao and D. Baskaran, Phys. Rev. D**79**, 083003 (2009); Phys. Rev. D**82**, 023001 (2010);
W. Zhao and L. P. Grishchuk, Phys. Rev. D **82**, 123008 (2010);
W. Zhao, Phys. Rev. D **79**, 063003 (2009); JCAP 1103:007, (2011).
- [46] T. P. Li, *et al.*, Mon. Not. R. Astron. Soc. **398**, 472 (2009).
H. Liu and T. P. Li, Astrophys. J **732**, 125 (2011).
- [47] W. H. Press and E. T. Vishniac, Astrophys. J. **239**, 1 (1980).
- [48] B. Ratra, Phys. Rev. D **38**, 2399 (1988).
- [49] L. P. Grishchuk, Phys. Rev. D**50**, 7154 (1994).
- [50] H.E. Jorgensen, E. Naselsky, P., Naselsky, and I. Novikov, Astron. & Astrophys, **294**, 639
(1995).
- [51] H. X. Miao and Y. Zhang, Phys. Rev. D **75**, 104009 (2007);
S. Wang, Y. Zhang, T.Y. Xia, and H.X. Miao, Phys. Rev. D **77**, 104016 (2008).
- [52] C. P. Ma and E. Bertschinger, Astrophys. J. **455**, 7 (1995)
- [53] S. Chandrasekar, *Radiative Transfer* , (Dover Publications, 1960), Chapter 1.
- [54] B. Keating, A. Polnarev, N. Miller, D. Baskaran, Int. J. Mod. Phys. A**21**, 2459 (2006)
- [55] P. J. E. Peebles, Astrophys. J. **153** (1968) 1.
- [56] P. J. E. Peebles, *Principles of Physical Cosmology* (Princeton University Press, Princeton,
1993)
- [57] R. A. Sunyaev and Ya. B. Zeldovich, Astrophys. Space Sci. **7**, 1 (1970).

- [58] B. J. T. Jones and R. F. G. Wyse, *Astron. Astrophys.*, **149**, 144, (1985).
- [59] P. J. E. Peebles and J. T. Yu, *Astrophys. J.* **162** 815 (1970).
- [60] M. Mortonson and W. Hu, *Astrophys. J.* **657**, 1 (2007).
- [61] D. D. Harari and M. Zaldarriaga, *Phys. Lett. B* **319**, 96(1993)
- [62] J. Silk, *Astrophys. J.* **151**, 459 (1968).
- [63] J. M. Bardeen, J. R Bond, N. Kaiser, and A. S. Szalay, *Astrophys. J.* **304**, 15 (1986).
- [64] A. H. Guth and S.-Y. Pi, *Phys. Rev. Lett.* **49**, 1110 (1982);
A. A. Starobinskii, *Phys. Lett. B***117**, 175 (1982);
S. W. Hawking, *Phys. Lett. B***115**, 295 (1982);
J. M. Bardeen, P. J. Steinhardt, and M. S. Turner, *Phys. Rev. D* **28**, 679 (1983).
- [65] F. Montanari, R. Durrer, *Phys. Rev. D* **84**, 023533 (2011).
- [66] P. Naselsky, and I. Novikov, *Astrophys. J.* **413**, 14 (1993).
- [67] N. Bartolo, S. Matarrese, A. Riotto, *JCAP* **0701** 019, (2007).
- [68] W. Hu and M. White, *Phys. Rev. D* **56**, 596 (1997).

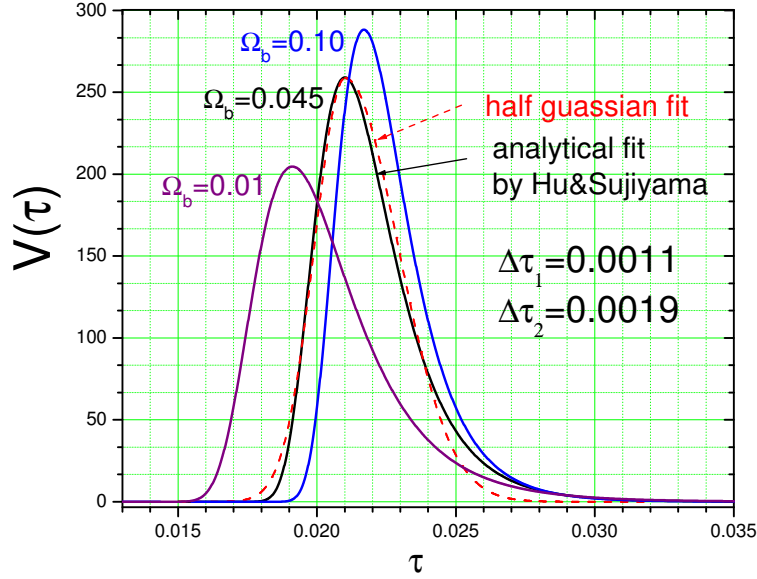


Figure 1: The visibility function $V(\tau)$ for the decoupling. The solid lines are given by the analytic formulae for different Ω_b from Ref.[40]. The dash line is the fitting by two pieces of half Gaussian functions as in Eq.(33).

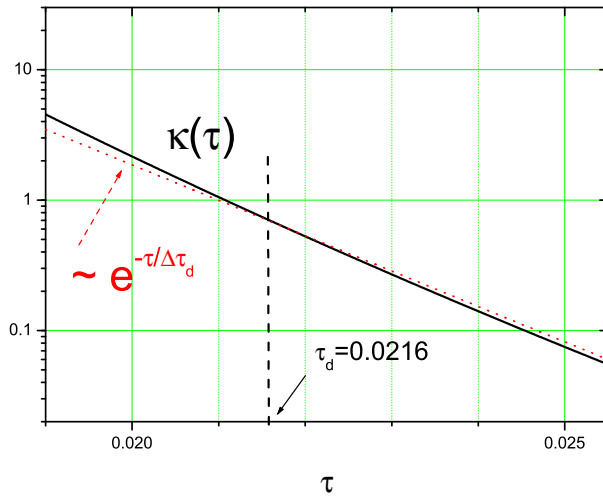


Figure 2: The optical depth function $\kappa(\tau)$ (solid) [40] can be approximated by a decreasing exponential function $\propto e^{-\tau/\Delta\tau_d}$ (dots) around the recombination.

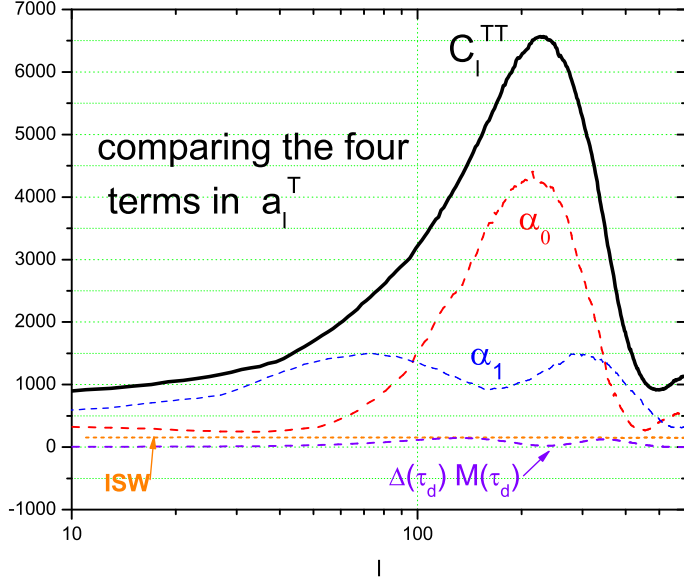


Figure 3: The multipole moment a_l^T has four terms in Eq.(78), which are schematically plotted for a comparison. α_0 is dominant at $l \sim 200$, α_1 is dominant at $l \lesssim 100$, the ISW is flat and low, and $\Delta\tau_d M(\tau_d)$ term is the lowest with two small bumps.

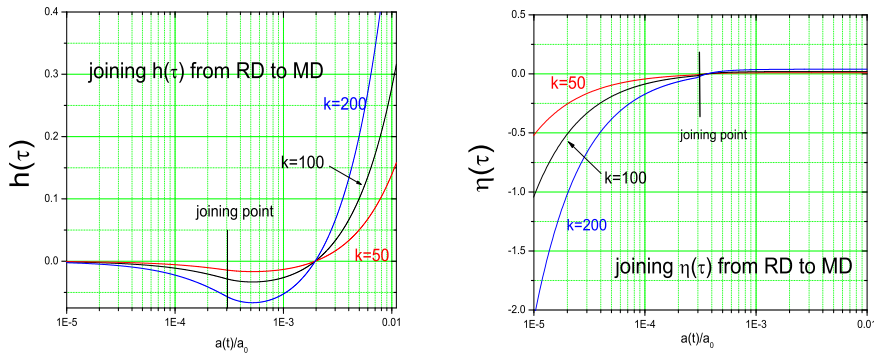


Figure 4: The perturbation modes $h(\tau)$ and $\eta(\tau)$ continuously joined at τ_2 , respectively.

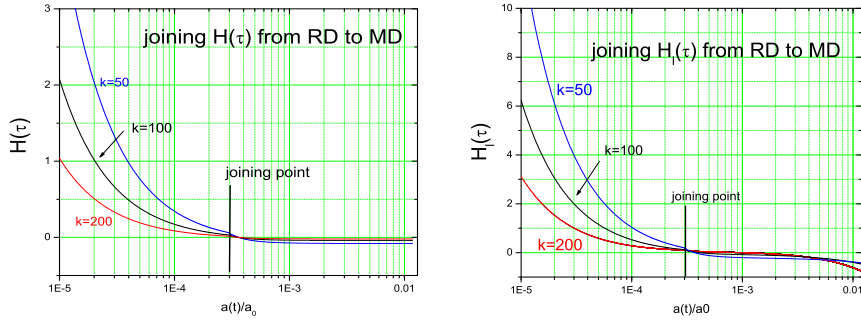


Figure 5: The perturbation modes $H(\tau)$ and $H_l(\tau)$ continuously joined at τ_2 , respectively.

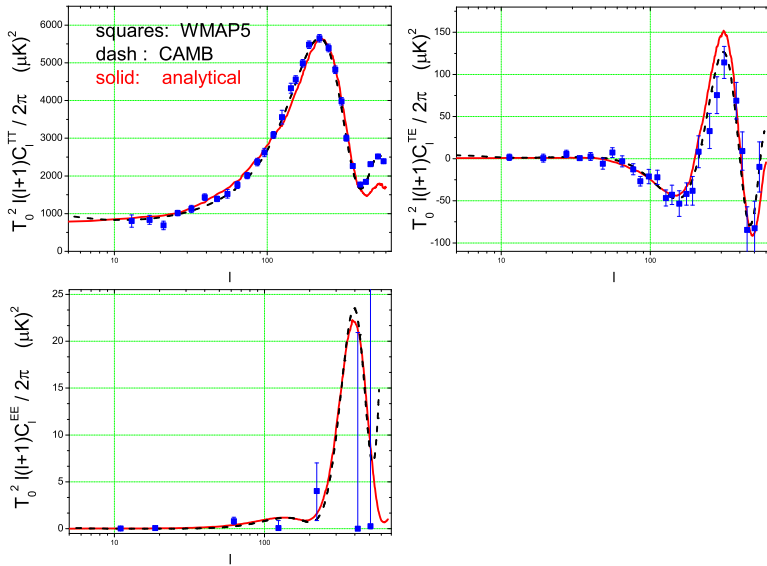


Figure 6: The analytical spectra (red line) $T_0^2 l(l+1)C_l^{XX'}/2\pi$ compared with the numerical result (dash lines) of CAMB [15] and the observed (square dots) WMAP5 [7].

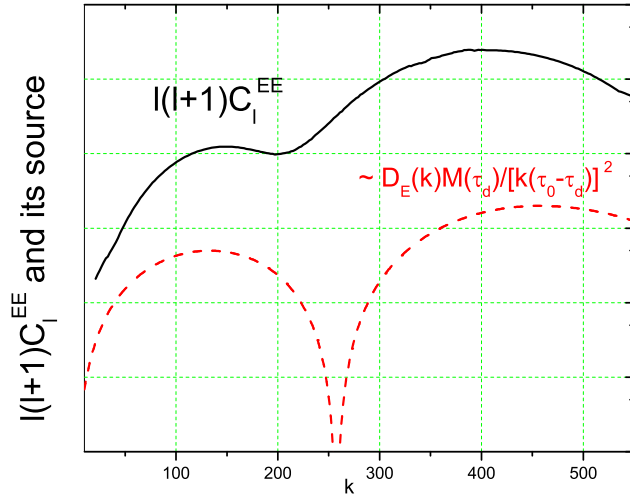


Figure 7: The profile of $l(l+1)C_l^{EE}$ (black line) is determined by its source $D_E(k)M(\tau_d)/(k(\tau_0 - \tau_d))^2$ in Eq.(69). In particular, the bump locations of $l(l+1)C_l^{EE}$ is determined by that of the scalar perturbations (red dotted line).

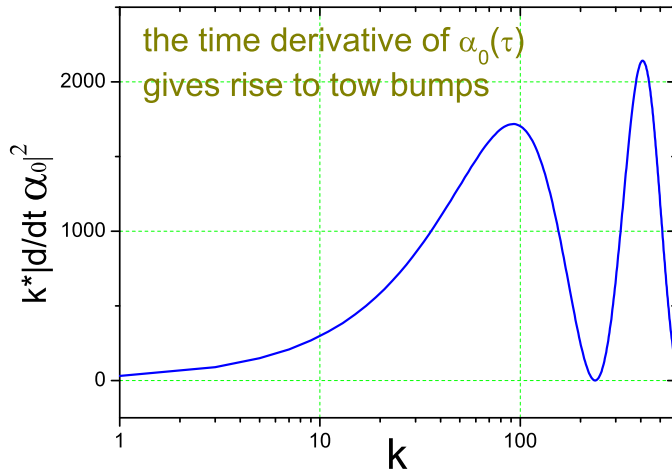


Figure 8: It is the time derivative $\dot{\alpha}_0(\tau)$ that gives rise to the first two bumps in C_l^{EE} .

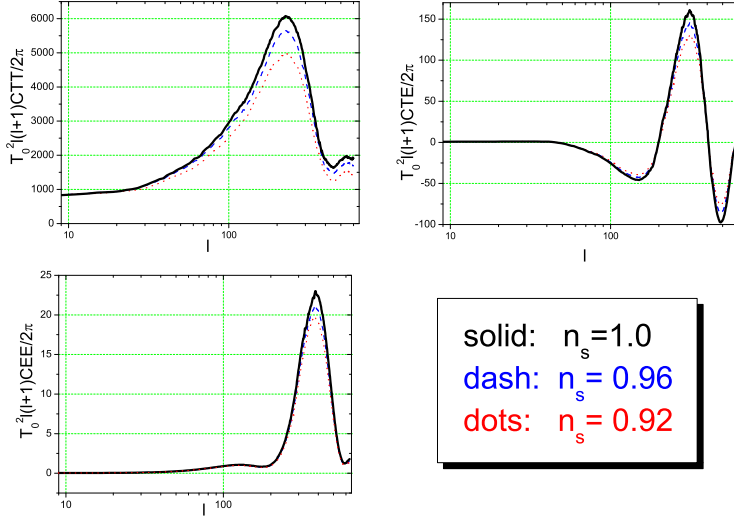


Figure 9: The spectra $C_l^{XX'}$ depend on the primordial power index n_s of the scalar metric perturbations.

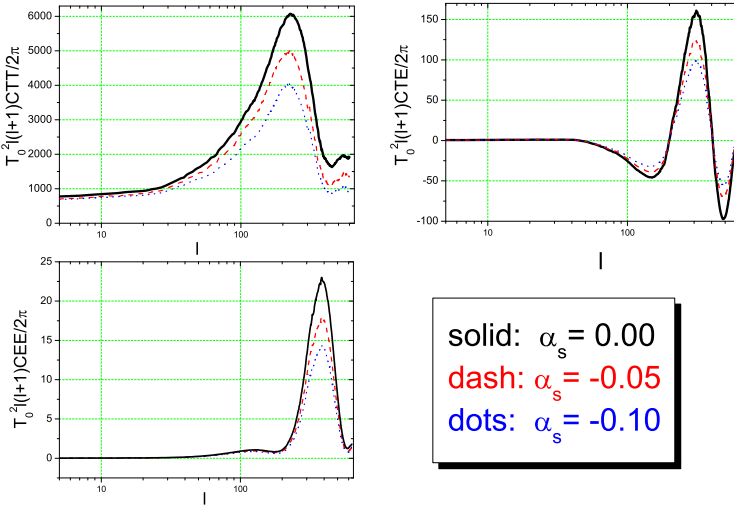


Figure 10: $C_l^{XX'}$ depend on the running index α_s of the scalar metric perturbations.

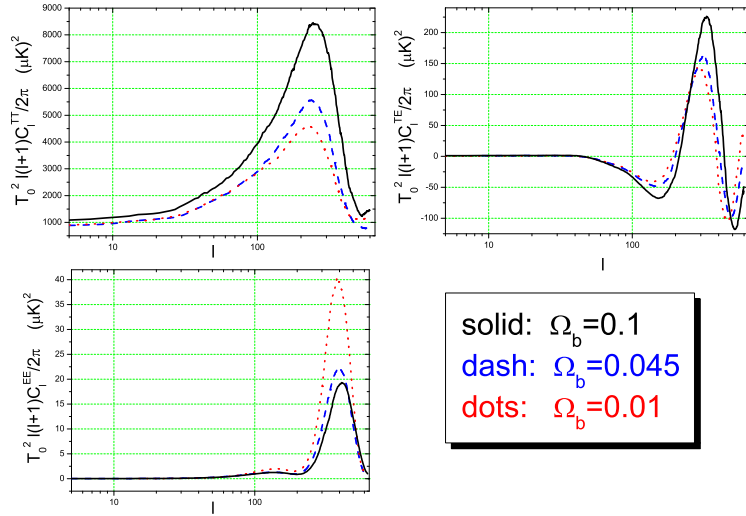


Figure 11: $C_l^{XX'}$ depend on the baryon fraction Ω_b .

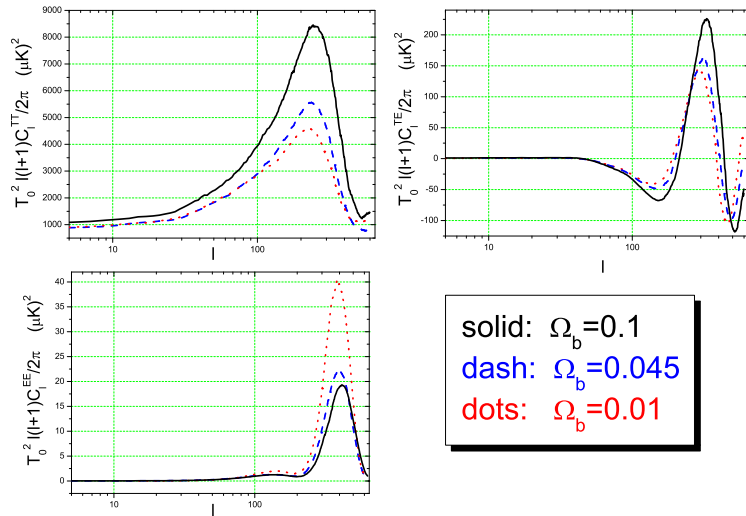


Figure 12: As the analytic expression tells, a longer recombination process (greater $\Delta\tau_d$) yields a higher amplitude of polarization C_l^{EE} , and brings more small-scale damping.

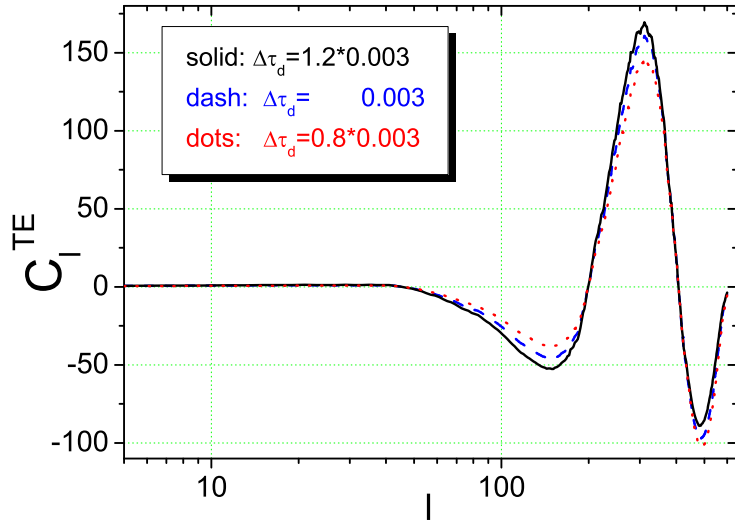


Figure 13: A longer recombination process yields higher peak and lower trough of cross-correlation C_l^{TE} .

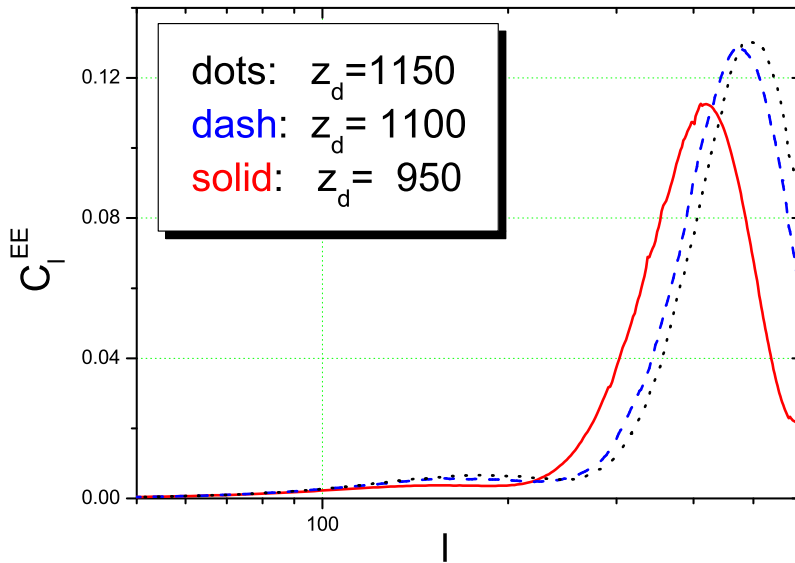


Figure 14: A late recombination time (larger τ_d) shifts the peaks and troughs of polarization to larger angular scales.

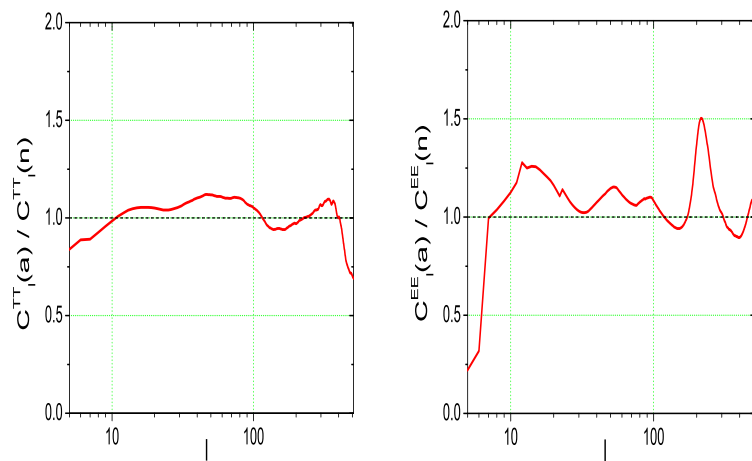


Figure 15: The ratio of the analytic spectra to numerical spectra. Left: $C_i^{TT}(a)/C_i^{TT}(n)$. Right: $C_i^{EE}(a)/C_i^{EE}(n)$.